HHS Public Access

Author manuscript

Cell Rep. Author manuscript; available in PMC 2023 November 27.

Published in final edited form as:

Cell Rep. 2023 October 31; 42(10): 113281. doi:10.1016/j.celrep.2023.113281.

Variable staphyloxanthin production by *Staphylococcus aureus* drives strain-dependent effects on diabetic wound-healing outcomes

Amy E. Campbell[1,5], **Amelia R. McCready-Vangi**[1,5], **Aayushi Uberoi**[1], **Sofía M. Murga-Garrido**[1], **Victoria M. Lovins**[1], **Ellen K. White**[1], **Jamie Ting-Chun Pan**[1], **Simon A.B. Knight**[1], **Alexis R. Morgenstern**[1], **Colleen Bianco**[3], **Paul J. Planet**[3,4], **Sue E. Gardner**[2], **Elizabeth A. Grice**[1,6,*]

[1]Departments of Dermatology and Microbiology, Perelman School of Medicine, University of Pennsylvania, Philadelphia, PA 19104, USA

[2]College of Nursing, University of Iowa, Iowa City, IA 52242, USA

[3]Division of Infectious Disease, Department of Pediatrics, The Children's Hospital of Philadelphia, Philadelphia, PA 19104, USA

[4]Departments of Pediatrics and Microbiology, Perelman School of Medicine, University of Pennsylvania, Philadelphia, PA 19104, USA

[5]These authors contributed equally

[6]Lead contact

SUMMARY

Strain-level variation in *Staphylococcus aureus* is a factor that contributes to disease burden and clinical outcomes in skin disorders and chronic wounds. However, the microbial mechanisms that drive these variable host responses are poorly understood. To identify mechanisms underlying strain-specific outcomes, we perform high-throughput phenotyping screens on *S. aureus* isolates cultured from diabetic foot ulcers. Isolates from non-healing wounds produce more staphyloxanthin, a cell membrane pigment. In murine diabetic wounds, staphyloxanthin-producing isolates delay wound closure significantly compared with staphyloxanthin-deficient isolates. Staphyloxanthin promotes resistance to oxidative stress and enhances bacterial survival in neutrophils. Comparative genomic and transcriptomic analysis of genetically similar clinical

*Correspondence: egrice@pennmedicine.upenn.edu.

AUTHOR CONTRIBUTIONS

Conceptualization, P.J.P., S.E.G., and E.A.G.; methodology, A.E.C., A.R.M.-V., S.M.M.-G., S.A.B.K., and V.M.L.; investigation, A.E.C., A.R.M.-V., A.U., S.M.M.-G., V.M.L., E.K.W., J.T.-C.P., S.A.B.K., A.R.M., and C.B.; visualization, A.E.C.; writing – original draft, A.E.C. and A.R.M.-V.; writing – review & editing, A.E.C., A.U., S.M.M.-G., V.M.L., E.K.W., J.T.-C.P., S.A.B.K., A.R.M., C.B., P.J.P., S.E.G., and E.A.G.; funding acquisition, P.J.P., S.E.G., and E.A.G.; supervision, S.A.B.K., P.J.P., and E.A.G.; resources, C.B., P.J.P., and S.E.G.

SUPPLEMENTAL INFORMATION

Supplemental information can be found online at https://doi.org/10.1016/j.celrep.2023.113281.

DECLARATION OF INTERESTS

The authors declare no competing interests.

isolates with disparate staphyloxanthin phenotypes reveals a mutation in the sigma B operon, resulting in marked differences in stress response gene expression. Our work illustrates a framework to identify traits that underlie strain-level variation in disease burden and suggests more precise targets for therapeutic intervention in *S. aureus*-positive wounds.

In brief

Campbell et al. investigate the phenotypic and genomic diversity of *S. aureus* isolates cultured from diabetic wounds. Production of staphyloxanthin, a yellow antioxidant pigment, associates with delayed healing. Identified as a mechanism underlying strain-specific outcomes in human diabetic wounds, staphyloxanthin promotes bacterial survival and impairs murine diabetic wound healing.

Graphical Abstract

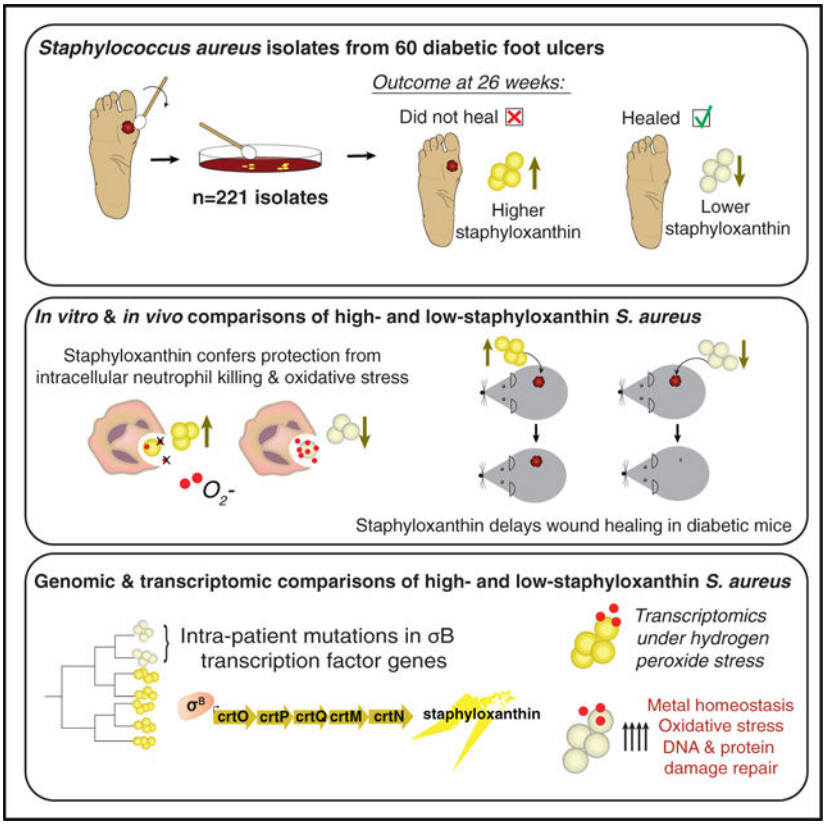

INTRODUCTION

Non-healing wounds are a common, costly, and debilitating complication of diabetes. The lifetime incidence of a diabetic foot ulcer (DFU) is estimated at 19%–34% in people with diabetes.[1] Treatment of lower-extremity complications is responsible for ~1/3 of total diabetic care costs, and standard treatment approaches include surgical debridement, offloading, and often local or systemic antimicrobials.[2,3] However, the prognosis for patients with DFUs remains poor, and DFUs account for two-thirds of all non-traumatic amputations

performed in the United States.[4,5] A DFU strongly increases the risk of death in those with diabetes, with 5-year mortality rates of 40%– 50%.[6,7] Despite the global healthcare burden posed by DFU complications, clinical management strategies have not evolved to meet the escalating need.

Many DFU complications owe to infections by contaminating bacteria, which colonize the wound bed. Of these microbes, the Gram-positive pathogen *Staphylococcus aureus* is the predominant bacterial species found in DFUs.[8,9] Highly prevalent across many types of cutaneous wounds, *S. aureus* is an important contextual pathogen that causes local and systemic infections that are difficult to treat.[10–13] Treatment for *S. aureus* is made more complicated by its evolving resistance to currently available antibiotics including methicillin and vancomycin.[8] Still, *S. aureus* can asymptomatically colonize the skin and nares, and its colonization of a DFU does not necessitate infection. Moreover, the culture-based presence or absence of *S. aureus* is not predictive of DFU healing outcomes.[14,15]

Rather, prior studies indicate that *S. aureus* effects on DFU healing are strain dependent and that uninfected and infected DFUs can be differentiated by virulence traits of colonizing *S. aureus* strains, which enable them to survive in the cutaneous wound environment and evade host immune responses.[16,17] Using shotgun metagenomics, we previously showed that specific strains of *S. aureus* populate healing vs. non-healing DFUs and that *S. aureus* exerts strain-specific effects on wound pathogenesis in a diabetic murine model.[18] In the same study, meta-genomic profiles from non-healing DFUs were enriched for *S. aureus* virulence- and pathogenicity-associated genes, including biofilm formation, as compared with healing DFUs. These and prior findings suggest that strain-level differences in *S. aureus* virulence factors contribute to delayed healing and other complications in DFUs.

S. aureus possesses an arsenal of virulence traits that vary between genetic lineages and may therefore help certain strains to infect the wound bed and impede healing. Though these virulence traits include secreted toxins that directly damage host tissues, they also include mechanisms by which *S. aureus* survives attacks from host cells and proliferates despite host-imposed limitations to bacterial survival. Biofilms, for example, entrench *S. aureus* in a resilient extracellular matrix, protecting it from antimicrobials and clearing by the host immune system.[19,20] Siderophores, which competitively bind environmental iron for uptake by *S. aureus*, enable it to overcome nutrient limitations inflicted by host iron sequestration.[21,22]

To evade innate immune detection and clearance, *S. aureus* produces proteins such as staphylokinase, which cleaves host plasminogen into plasmin, enabling the clearance of opsonic host factors such as immunoglobulin G (IgG) and C3b from the wound bed.[23] In the highly oxidative diabetic wound environment, *S. aureus* can suffer substantial damage to its proteins and genetic material.[24,25] To prevent and mitigate this damage, *S. aureus* deploys stress resistance factors such as the carotenoid pigment staphyloxanthin, which neutralizes reactive oxygen species (ROS) such as those produced by host neutrophils.[26,27] Such virulence factors are likely essential to *S. aureus* survival and proliferation in the diabetic wound environment. However, it remains unclear which protective phenotypes most

strongly determine DFU outcomes and how these phenotypes enable certain strains of *S. aureus* to cause tissue damage and delay healing in a diabetic wound context.

To address this gap, we employed a collection of 221 *S. aureus* clinical isolates cultured from a longitudinal prospective study of wound bioburden in 100 neuropathic DFUs.[14] We characterized virulence in the resulting *S. aureus* isolate collection using high-throughput screens for traits that confer *S. aureus* resistance to host immune attacks. DFU isolates from non-healing wounds were enriched in production of the antioxidant pigment staphyloxanthin. By leveraging clinical isolates with variable staphyloxanthin phenotypes and transposon mutants, we found that staphyloxanthin contributes to delayed wound healing in a diabetic murine model. Staphyloxanthin-producing strains showed enhanced neutrophil recruitment *in vivo*, were more resistant to oxidative stress *in vitro*, and survived intracellularly in neutrophils *in vitro*. Using whole-genome sequencing and comparative genomics of high- and low-staphyloxanthin-producing isolates, we identified a mutation that attenuated staphyloxanthin production via a regulator of sigma B, an alternative sigma factor involved in *S. aureus* stress response. Transcriptomic comparisons revealed that in response to peroxide stress, a clinical isolate with the mutation exhibited greater upregulation of oxidative stress response genes and protein damage repair genes compared with a high-staphyloxanthin clinical isolate lacking the mutation. Finally, a preliminary comparative genomic analysis on the sequenced *S. aureus* isolates revealed multiple intrahost mutations in sigma B operon genes that correlated with low staphyloxanthin production, suggesting that despite being essential to *S. aureus* survival in neutrophils and impairment of DFU healing, staphyloxanthin may be an early and acute, rather than chronic and persistent, phenotype for *S. aureus*.

RESULTS

Phenotypes of *S. aureus* in a culture collection from human DFUs

To identify factors that may underlie *S. aureus* strain-level variation in DFU healing outcomes, we used a collection of *S. aureus* isolates from a previously described longitudinal prospective cohort study of DFU bioburden and association with clinical outcomes.[14] Enrolled subjects presented with plantar, neuropathic DFUs lacking signs of clinical infection and underwent sharp debridement followed by offloading. DFUs were monitored biweekly for 26 weeks or until healed or amputated, with wound swab specimens collected at each visit (Figure 1A). Swabs were plated under a range of media conditions, including *S. aureus*-selective chromogenic detection plates. Sixty DFUs were positive for *S. aureus* at some time point during the 26-week study, yielding 221 total *S. aureus* isolates. Of the 60 DFUs that were *S. aureus* culture positive, 43 healed by the end of the study (72%) (Figure 1A). Roughly similar numbers of *S. aureus* isolates were obtained from DFUs that healed (n = 108) vs. DFUs that did not heal by the end of the study (n = 113). As reported in the original study, there was not a significant difference in the presence of cultured *S. aureus* and DFU healing outcome.[14]

To characterize variation in the 221 *S. aureus* isolates in this collection, we selected four well-characterized stress-and immune-responsive phenotypes that are quantifiable in high throughput: biofilm formation (Figure 1B), siderophore production (Figure 1C),

staphylokinase activity (Figure 1D), and staphyloxanthin production (Figure 1E). The distribution of phenotypes by isolate for all *S. aureus* isolates from healed (left) and unhealed (right) DFUs by the end of the 26-week study are depicted in Figures 1B–1EI (see also Table S1). Because some isolates came from the same DFU and/or time point, we de-duplicated the dataset for statistical analysis by selecting the highest-virulence isolate for each virulence phenotype in each DFU.

We assessed *in vitro* biofilm formation using an adapted crystal violet staining technique.[28] Although *S. aureus* isolates varied in ability to form biofilm, isolates obtained from non-healing DFUs did not produce significantly more biofilm *in vitro* than isolates from DFUs that healed by the end of the 26-week study ($p = 0.4957$; Figure 1Bii). Siderophore production, quantified by measuring iron depletion in the presence of *S. aureus* supernatants, was also variable but did not differ between healed and unhealed DFUs ($p = 0.775$; Figure 1Cii).[29]

We quantified staphylokinase activity in all isolates using a plasmin-specific chromogenic substrate that is activated when staphylokinase cleaves exogenously added human glu-plasminogen into plasmin.[30] We observed that there was no significant difference in staphylokinase activity when comparing isolates from healed and unhealed DFUs ($p = 0.2622$; Figure 1Dii).

The carotenoid pigment staphyloxanthin was extracted from liquid cultures via methanol and quantified colorimetrically. Isolates from non-healing DFUs produced significantly more staphyloxanthin compared with isolates from DFUs that healed ($p = 0.0089$; Figure 1Eii). Similar results were obtained when comparing isolates from DFUs that did or did not heal by 12 weeks, a time point that is commonly used to distinguish chronic non-healing DFUs ($p = 0.0042$) (Figure S1). Staphyloxanthin was also the phenotype most strongly associated with healing outcome when comparing the median ($p = 0.0317$) and mean ($p = 0.0694$) phenotype measure by patient (Figure S1).

In addition to comparing each phenotype in deduplicated isolates from healing and non-healing patients using t tests (Figures 1Bi, 1Ci, 1Di, and 1Ei), we fit a multilevel linear mixed model (LMM) for each phenotype of the form $Phenotype \sim (1|patient) + HealingOutcome$, where *Phenotype* is the min-maxnormalized mean phenotype measure for an isolate across biological and technical replicates, *patient* is the patient ID, and *HealingOutcome* represents healed or unhealed status at the end of the study.[31] Of the four phenotype models, staphyloxanthin displayed the strongest relationship to the healing outcome factor of the four phenotypes in a well-fitting model (Table S3). Collectively, these data demonstrate an association between increased staphyloxanthin production by *S. aureus* and poor clinical outcome of DFUs.

Staphyloxanthin promotes *S. aureus* survival under oxidative conditions

To further examine the association between staphyloxanthin and delayed healing, we looked at the distribution of staphyloxanthin production among isolates from each individual DFU (Figure 2A). One non-healing DFU in particular, DFU141, presented with a unique staphyloxanthin profile: of the 14 *S. aureus* isolates obtained from DFU141 over the

course of 16 weeks, 11 produced distinctly high and 3 produced distinctly low levels of staphyloxanthin (Figure 2B). This observation among DFU141 *S. aureus* isolates motivated a case study of dichotomous staphyloxanthin production in a subset of our clinical isolates. We selected representative isolates with the highest and lowest staphyloxanthin production from this DFU for in-depth analysis: SA925 and SA1088, respectively (Figure 2B).

To isolate the effects of staphyloxanthin alone, we obtained the USA300 *S. aureus* strain JE2 and a transposon mutant of the *crtN* gene in JE2 (JE2-crtN::Tn; Figure 2C).[32] The *crtN* gene encodes the dehydrosqualene desaturase enzyme, a critical enzyme in staphyloxanthin biosynthesis, and part of the *crt* operon, which encodes for staphyloxanthin production.[33] A *crtN* transposon mutant produces virtually no staphyloxanthin, significantly less than JE2 ($p = 0.0062$; Figure 2D). Similarly, in the clinical isolate comparison, SA925 produced significantly more staphyloxanthin than SA1088 ($p = 0.0032$; Figure 2D). To inhibit staphyloxanthin production in clinical isolates, we used thymol (2-Isopropyl-5-methylphenol), a monoterpene alcohol isolated from the plant *Thymus vulgaris.* Thymol selectively inhibits staphyloxanthin production in *S. aureus* via binding to CrtM (Figure 2C), the first enzyme in the staphyloxanthin biosynthesis pathway.[34] The addition of thymol (100 ¼M) robustly abrogated staphyloxanthin production in both high-staphyloxanthin-producing isolates, JE2 and SA925 (Figure 2E).

Staphyloxanthin promotes *S. aureus* survival by providing protection from oxidative stress inflicted by the host immune system.[27] To test this in our isolates, we performed *in vitro* hydrogen peroxide (H_2O_2) challenge assays, with the rationale that higher staphyloxanthin production would increase the survival of *S. aureus* when exposed to 3% H_2O_2. Survival of JE2 was significantly higher than the JE2-crtN::Tn mutant (colony-forming unit [CFU] survival = 113% vs. 35%; $p = 0.024$); similarly, survival of the clinical isolates reflected their staphyloxanthin production (CFU survival = 104% SA925 vs. 20% SA1088; $p = 0.0055$) (Figure 2F). Growth curves (8 h) in planktonic culture were similar across all four isolates, suggesting that differential growth rates were not responsible for this result (Figure S2A). The survival differences between high- and low-staphyloxanthin producers in both clinical and JE2 control strains suggest that staphyloxanthin production contributes to *in vitro* oxidative stress resistance.

To determine whether enhanced survival in SA925 and JE2 was due to staphyloxanthin production, as opposed to other stress responses, the isolates were grown in the presence of 100 mM thymol and then exposed to 3% H_2O_2. This resulted in a significant drop in survival for JE2 (27%; $p = 0.0143$) and SA925 (35%; $p = 0.0053$) (Figure 2F). Furthermore, when grown with thymol, their survival was no longer significantly greater than JE2-crtN::Tn and SA1088, respectively (Figure 2F). To confirm that the pigment and H_2O_2 survival advantage of JE2 compared with JE2-crtN::Tn is due to the interruption of *crtN* and not secondary mutations, we complemented a functional *crtN* gene back into JE2-crtN::Tn using the xylose-inducible pEPS5A plasmid vector, modified to include JE2's own *crtMN* region to yield the JE2-crtN::Tn/pEP-crtMN strain.[35,36] In addition to restoring pigmentation to JE2-crtN::Tn (Figures 2H and S2B), this complemented mutant also survived exposure to 0.3% hydrogen peroxide as well as the parent strain JE2 ($p = 0.5653$, Figure 2I). Together, these

results suggest that the survival differences observed between the strains under oxidative stress are due to differences in staphyloxanthin production.

Staphyloxanthin can increase bacterial cell membrane stability by ordering the alkyl chains of membrane lipids, thus enhancing *S. aureus* survival of membrane-disrupting antibiotics.[37] To test membrane stability, we exposed *S. aureus* isolates to polymyxin B (1 mM), a membrane-disrupting antibiotic. We observed a moderate decrease in survival with polymyxin B exposure in JE2-crtN::Tn and SA1088 as compared with the staphyloxanthin-producing isolates JE2 and SA925, respectively, though these findings were not statistically significant, and we observed substantial variability in survival among both SA925 and JE2 replicates (Figure 2G). Therefore, we cannot conclude whether membrane stability is substantially different between these strains.

Staphyloxanthin impairs *in vivo* wound healing in a diabetic murine model

To determine whether staphyloxanthin production by *S. aureus* has an *in vivo* effect on diabetic wound healing, we employed a murine model of diabetes in which mice lack the leptin receptor $Lepr^{db/db}$ (referred to as db/db subsequently).[38] In a pilot experiment in db/db mice, infection with high-staphyloxanthin-producing clinical isolate SA925 significantly delayed healing compared with low-staphyloxanthin-producing SA1088 or PBS control (Figure S3A). Guided by these preliminary studies, we designed two independent wound-healing experiments in male and female 12-week-old db/db mice. Excisional 8-mm full-thickness dorsal wounds were inoculated with 2×10^8 CFU JE2, JE2-crtN::Tn, SA925, SA1088, or vehicle control (PBS+10% glycerol) and covered with Tegaderm. Wounds were photographed and measured at days 0, 3, 7, and 14 in both experiments.

We compared wound closure among mice treated with *S. aureus* isolates and controls to determine whether staphyloxanthin influences diabetic wound healing. A representative image for each group and time point is shown in Figure 3A. All *S. aureus* strains impacted wound-closure dynamics to some degree, but staphyloxanthin-producing strains exacerbated delayed healing (Figure 3B). At experimental day 14, wounds exposed to JE2 were significantly larger than wounds exposed to JE2-crtN::Tn ($p = 0.0114$; Figure 3C). Furthermore, wounds exposed to the high-staphyloxanthin-producing clinical isolate SA925 were significantly larger than wounds exposed to SA1088 ($p = 0.00074$; Figure 3C). We also observed that female mice were significantly delayed in healing at 14 days post-wounding compared with male mice ($p = 0.031$), suggesting a sex bias in *S. aureus* infection and/or diabetic wound healing. We observed that strain SA925 caused mortality in 4 mice over the course of the 3 experiments described above, whereas no mice exposed to SA1088 died prior to the experimental endpoint (Figure S3B).

Having observed significant healing deficiencies in both SA925-compared with SA1088-infected mice and JE2-compared with JE2-crtN::Tn-infected mice, we measured the CFUs recovered from tissue biopsies at experimental endpoints. At day 21, *S. aureus* CFUs from wound tissue were not significantly different between SA925/SA1088 or JE2/JE2-crtN::Tn (Figure S3D). Because infection experiments in other disease contexts have shown the importance of sigma B-dependent phenotypes at early stages of infection, we repeated the wounding experiment to measure tissue CFUs at days 7 and 3.[39] We recovered significantly

higher levels of *S. aureus* in SA925-than SA1088-infected mice at days 7 and 3 ($p = 0.0074$, $p = 0.0054$) but did not recover significantly different *S. aureus* CFUs from JE2 vs. JE2-crtN::Tn ($p = 0.4948$, $p = 0.9581$). While SA925 shows a clear survival advantage in our model over the staphyloxanthin-deficient SA1088, we cannot conclude JE2's improved survival over JE2-crtN::Tn based on CFU counts alone. However, the clear delay in wound healing in JE2-infected over JE2-crtN::Tn-infected and SA925-infected over SA1088-infected mice indicates that increased staphyloxanthin production by *S. aureus* contributes to delayed wound healing in this murine model of diabetic wound infection.

Staphyloxanthin promotes survival from neutrophils and recruitment to wounded skin

Neutrophils are important for bacterial control and can kill *S. aureus* by engulfing and exposing the bacteria to ROS via the activity of myeloperoxidase and NADPH oxidase.[40] Staphyloxanthin protects *S. aureus* from intracellular neutrophil killing, thus promoting host immune evasion.[27] We therefore hypothesized that the differences we observed in murine diabetic wound healing were a result of staphyloxanthin-mediated protection from neutrophil recognition and/or clearance. We first quantified the survival of *S. aureus* clinical isolates and lab strains in whole human blood, an assay that measures opsonophagocytic killing by peripheral blood neutrophils. We exposed 1×10^4 CFUs of each JE2, JE2-crtN::Tn, SA925, and SA1088 to freshly drawn whole human blood for 4 h before plating and quantifying CFUs. Survival of JE2 was significantly greater than that of the staphyloxanthin mutant JE2-crtN::Tn ($p = 0.049$; Figure 4A). Similarly, survival of SA925 was greater than SA1088, though not significantly so ($p = 0.1181$; Figure 4A). These results suggest that staphyloxanthin partially protects *S. aureus* from opsonophagocytic killing in human blood.

To examine the role of staphyloxanthin in *S. aureus* intracellular neutrophil survival, we performed a neutrophil survival assay by exposing freshly isolated primary human neutrophils to *S. aureus*. The neutrophils were then washed to remove any extracellular bacteria and lysed so bacterial CFUs could be quantified. We observed increased survival of high-staphyloxanthin-producing strains JE2 and SA925 compared with low-staphyloxanthin producers JE2-crtN::Tn and SA1088 ($p = 0.0358$ and $p = 0.0103$, respectively; Figure 4B). These results support the claim that staphyloxanthin specifically enhances intracellular *S. aureus* survival in human neutrophils.

Because staphyloxanthin is a cell surface molecule, we reasoned that it may also contribute to neutrophil recruitment and persistence in wound tissue. To test this, we employed an ear wound model, where a 2-mm hole punch is created in the center of the outer ear pinna in C57BL6/J mice.[41] Punch wounds were treated with *S. aureus* clinical isolates SA925, SA1088, or vehicle control for 1 week. The ear pinnae were collected, and flow cytometry was performed to assess immune cell populations in the tissue (Figure S4). As measured by Ly6G+CD11b+ cells, a significantly higher percentage of neutrophils infiltrated tissue exposed to SA925 compared with both SA1088 and control ($p = 10^{—4}$ and $p = 0.0057$, respectively; Figure 4D; Table S3). In a separate experiment, we repeated this model with JE2 vs. the staphyloxanthin-deficient JE2-crtN::Tn and observed higher neutrophil

recruitment with either strain than the punch control but observed no significant difference between mice infected with JE2 and JE2-crtN::Tn ($p = 0.4083$; Figure 4C).

To determine whether these results would be consistent in the context of diabetes, we repeated the experiment with diabetic (db/db) mice. Overall, the directional trends were consistent with our observations in non-diabetic mice, though neutrophil differences between SA1088 and SA925 in db/db mice were not statistically significant ($p = 0.1266$; Figure 4F; Table S3). We observed a stronger deficiency in neutrophil recruitment in JE2-crtN::Tn-infected mice compared with JE2 mice in the diabetic mouse model, though this difference also failed to meet an $\alpha = 0.05$ threshold ($p = 0.0781$; Figure 4E). Though these experiments showed variation between replicate mice, they support a role for staphyloxanthin in the recruitment of neutrophils to wound tissue.

Whole-genome comparisons between high- and low-staphyloxanthin isolates in DFU141 identify a single-nucleotide variant in the *rsbU* regulator of sigma B

To determine the genomic differences underlying the disparate staphyloxanthin phenotypes observed in the 14 isolates cultured from DFU141, we employed whole-genome sequencing, comparative genomic, and phylogenetic approaches. To compare genomes at the highest structural and sequence-level resolution, we sequenced all 14 isolates using Illumina short-read sequencing followed by Oxford Nanopore long-read sequencing on 13/14 isolates to use as structural scaffolds for the short reads during hybrid genome assembly.

We classified the 14 assembled genomes as belonging to the CC1 lineage of *S. aureus* based on PubMLST.[42] We annotated each genome using Prokka and estimated their core and accessory genomes using Roary, including the CC1 MW2 reference genome as a closely related outgroup.[43,44] An estimated maximum likelihood phylogeny grouped the three low-staphyloxanthin-producing isolates together in a monophyletic clade (Figure 5A), suggesting that this genotype/phenotype combination may have arisen intrahost. The DFU141 isolate genomes were very genetically similar, as shown by their pairwise average nucleotide identity (ANI) compared with three other CC1 reference genomes (Figure 5B). We performed pairwise alignments and comparisons of the 14 genomes for structural variants, single-nucleotide polymorphisms (SNPs), and large-scale insertions/deletions using NucDiff.[45] These comparisons identified exactly three SNPs and one 9-base deletion, which were consistently present in low-staphyloxanthin genomes but absent from high-staphyloxanthin genomes (Figure 5A). Of these four consistent variants, one SNP and the deletion were predicted by both Prokka and PGAP annotations to be in non-coding regions.[46] One SNP corresponding to a Thr→Ala amino acid change was predicted by PGAP to be in a hypothetical open reading frame (ORF) between *folK* and *LysS* but was predicted by Prokka to be in a non-coding region. The fourth SNP was located in the positive sigma B regulator *rsbU*, corresponding to a Met→Leu amino acid change in the active phosphatase domain of *rsbU* (Figure 5A).

The *rsbU* gene encodes a well-characterized phosphatase regulator of the sigma B operon that, in response to environmental stress, dephosphorylates RsbV, which prevents inhibition of sigma B by RsbW (Figure 5C).[47] The transcription factor sigma B, in turn, positively regulates the *crt* biosynthetic operon for staphyloxanthin. Along with the fact that this

non-synonymous SNP corresponds to an amino acid change in the catalytic domain of the protein, the *rsbU* variant is most likely responsible for impaired staphyloxanthin production in DFU141 isolates. Consistent with previous studies, we found that *rsbU* was necessary for staphyloxanthin production (Figure S5A).[48] Still, this variant represents a change in protein sequence that may alter, but not necessarily abolish, RsbU's regulatory function. This motivated our subsequent investigation into the transcriptomic differences between high- and low-staphyloxanthin DFU141 isolates and how the two strains respond to oxidative stress at the transcriptional level.

Though the four genetic variants summarized in Figure 5A were the only ones consistently present in the 3 low-staphyloxanthin-producing isolates and absent from the 11 high-staphyloxanthin-producing isolates, there were other pairwise differences among isolates. For example, the representative staphyloxanthin-producing isolate SA925 contains a phage insertion absent from SA1088 with >99% nucleotide identity to the φSa3mw phage from *S. aureus* MW2 (GenBank: BA000033.2), which contains staphylokinase (*sak*), staphylococcal complement inhibitor (*scn*), and staphylococcal enterotoxins a and q (*entQ* and *entA*, respectively), among other phage-associated genes.[49]

Staphyloxanthin alters expression of stress response genes under oxidative stress conditions and protects *S. aureus* from oxidative damage

We investigated transcriptional differences between the high- and low-staphyloxanthin-producing isolates from DFU141 when exposed to oxidative conditions. To evaluate this, we conducted RNA sequencing (RNA-seq) analysis on SA925 and SA1088 with and without 1% H_2O_2 exposure. Consistent with our comparative genomic analysis indicating that the low-staphyloxanthin phenotype in DFU141's SA1088, SA1000, and SA1038 is likely due to disrupted RsbU and therefore sigma B regulatory function, multiple genes previously shown to be positively regulated by sigma B are upregulated in SA925 compared with in SA1088, including *asp23* and *clfA*.[39,50] Under H_2O_2 exposure, expression of genes in the *crt* operon was significantly higher in SA925 compared with in SA1088 (Figure 5D). Consistent with previous reports, under H_2O_2 stress, sigma B (*sigB*) operon genes were generally downregulated in both strains but more significantly so in SA1088.[51,52] The exception was *rsbU*, which was significantly more downregulated in SA925 compared with in SA1088 (Figure 5D).

Quorum sensing operon *agrABCD* was more highly expressed in SA925 compared with in SA1088 under H_2O_2 conditions. Interestingly, *agrABCD* was upregulated in SA1088 in response to H_2O_2. This coincided with H_2O_2-responsive downregulation of *rsbU* in SA1088, suggesting that while SA1088's mutant *rsbU* may be incapable of adequate *sigB* activation to promote *crt* expression, it may still be able to downregulate *agr* as previously reported.[53]

We hypothesized that stress response genes, and in particular those responsible for mitigating oxidative stress, would be upregulated in response to H_2O_2. Indeed, we observed that the expression of a number of stress response genes increased significantly under these conditions in both isolates, including *sodA*, *tpx*, *trxA*, *nfrA*, and *sarA* (Figure 5C). Interestingly, we found that several oxidative stress sensing and resistance genes were significantly upregulated in SA1088, but not in SA925, including *ahpC*, *perR*, *lytM*, and

walR. These genes could offer compensatory resistance mechanisms to the oxidative stress responses impeded by the *rsbU/sigB* defect in SA1088. SA1088 also uniquely upregulated several metal homeostasis genes in the presence of H_2O_2 compared with SA925, including *isdB*, *isdI*, *mgrA*, and multiple staphyloferrin B (*sbn*) operon genes. Both strains exhibited changes in expression of DNA damage repair genes in response to H_2O_2, though SA1088 uniquely upregulated the endonuclease *nth*, while SA925 uniquely upregulated *polX*, *addA*, and *uvrA*. Furthermore, SA1088 upregulated more genes related to damaged protein repair and degradation, including the *clpC* operon, *msrAB*, and *sufAB*.[54,55] This suggests that SA1088, deficient in staphyloxanthin and other SigB-dependent stress resistance traits, may incur more damage to its proteins by H_2O_2, necessitating the activation of these protein repair and degradation pathways.

In addition to different stress responses, we observed several toxicity-associated genes to be expressed more highly in SA925 compared with in SA1088 under both conditions (Figure S5B). Though *entA*, entQ, *sak*, and *scn* are all found on the MW2 phage and therefore missing from SA1088, only *scn* was upregulated in SA925 in response to H_2O_2 exposure. Other toxicity genes not found on the MW2 phage insertion were more highly expressed in SA925 than in SA1088 despite their presence in both strains, including phenol-soluble modulin components (*psmα1–4*) and delta hemolysin (*hld*). While none of these genes were upregulated in either strain in response to H_2O_2, alpha and gamma hemolysins (*hly*, *hlgC*, *hlgB*) were upregulated in both SA1088 and SA925 in response to H_2O_2 exposure.

Overall, there were more stress response genes upregulated in SA1088 compared with in SA925 under H_2O_2 conditions, particularly those related to iron uptake and storage, damaged protein repair and degradation, and oxidative stress mechanisms other than staphyloxanthin. These findings suggest that the staphylox-anthin-deficient *rsbU* mutant SA1088 experiences greater stress in response to SA925. This is consistent with our findings that high-staphyloxanthin strains experience greater H_2O_2 survival and suggests that staphyloxanthin embedded in the *S. aureus* cellular membrane protects it from oxidative stress.

Loss-of-function mutations in the sigB operon may be a convergent source of variation in staphyloxanthin production

Similar to our observations in isolates collected longitudinally from DFU141, loss-of-function mutations in sigB operon genes have previously been reported in staphyloxanthin-deficient clinical isolates of *S. aureus* collected from cystic fibrosis and soft-tissue infections.[52,53,56] To explore whether the loss-of-function *rsbU* mutation observed in DFU141 is exemplary of a common source of staphyloxanthin variation in DFUs over time, we performed a preliminary comparative analysis of the amino acid sequences for genes in the sigB operon (*rsbU-rsbV-rsbW-sigB*) in 206 additional isolates from the remaining 59 patients (Figure 6A). We found 5 additional DFUs that contained isolates with non-synonymous mutations in *rsbU*, *sigB*, or *rsbW* and produced lower staphyloxanthin than isolates from the same DFU belonging to the same *S. aureus* clonal complex (CC). In particular, we found three such examples in just *rsbU*, one in just *rsbW*, and one example of an *S. aureus* strain with amino acid substitutions in both *sigB* and *rsbW*. Of these 5 variants,

4 were found exclusively in isolates collected at week 4 or later. Together with DFU141, this amounts to 5 DFUs with potential intrahost loss-of-function mutations in the sigB operon, 3 of which failed to heal by the end of the study period.

Given that these findings would imply the loss of the staphyloxanthin phenotype within the DFU time course, we asked whether staphyloxanthin production was higher in isolates collected at earlier time points. Indeed, among only DFUs that did not heal by the end of the study period, we found a strong negative correlation ($r = —0.273$, $p = 0.0129$) between staphyloxanthin levels and the time point at which isolates were collected. There was no correlation between staphyloxanthin and time point among DFUs that healed (Figure 6B). These results suggest that although staphyloxanthin is essential in delaying DFU healing by establishing an infection, it may be most valuable to *S. aureus* at early, inflammatory wound phases, when it needs to overcome attacks from host immune cells to establish an infection. This is consistent with our observation that wounds infected with SA925 yielded higher *S. aureus* CFUs than *rsbU* mutant SA1088 at days 3 and 7 but not at day 21 (Figure S3).

DISCUSSION

S. aureus is a common pathogen to injured skin and wounds, and particular strains of *S. aureus* have been shown to delay diabetic wound healing. Because the *S. aureus* phenotypes that contribute to poor healing and infection-related wound outcomes are not well defined, we sought to identify strain-dependent *S. aureus* factors associated with poor healing outcomes. We performed high-throughput phenotyping screens on a collection of 221 *S. aureus* isolates from 60 DFUs. We discovered that production of the pigment staphyloxanthin was associated with delayed healing (Figure 1). These results led us to hypothesize that staphyloxanthin may contribute to *S. aureus* strain-level variation in DFU outcomes.

We then compared representative high- and low-staphyloxanthin-producing isolates (SA925 and SA1088, respectively) from a single wound (DFU141) to explore the mechanistic interactions between staphyloxanthin and the host immune system. We addi- tionally employed the laboratory strain JE2 and its mutant JE2crtN::Tn in parallel to isolate the effects of staphyloxanthin production and to compare them with the effects of a naturally occurring mutation in the sigB regulatory pathway. Additionally, we showed that complementing *crtMN* back into the JE2-crtN::Tn mutant restores both its pigmentation and its resistance to H_2O_2 stress (Figures 2H and 2I).

Despite the genetic similarity between SA925 and SA1088, RNA-seq analysis revealed substantial gene expression differences, with and without exposure to H_2O_2. SA1088 upregulated more genes involved in iron transport and storage under H_2O_2 stress compared with SA925 (Figure 5D). This is consistent with previously elucidated relationships between iron homeostasis and oxidative stress in *S. aureus*, including a previous study demonstrating that a *rsbU* mutant form of the *S. aureus* MW2 strain upregulated iron storage and transport genes in response to H_2O_2 stress.[51,57] Simultaneously, SA1088 upregulated many genes responsible for repairing stress-induced protein damage and targeting damaged proteins for degradation (Figure 5C), suggesting that SA1088 is more vulnerable to oxidative damage by

H_2O_2 than SA925. Collectively, these findings suggested that the *rsbU* mutant SA1088 was more susceptible to oxidative stress than the non-mutant, high-staphyloxanthin-producing SA925 strain.

We observed that SA925 expressed lower levels of *rsbU* under H_2O_2 stress compared with SA1088, which carries a mutation in the phosphatase domain. We hypothesize that SA1088 compensates for its mutation by upregulating *rsbU*. This hypothesis is supported by our finding that the *agr* quorum sensing system is significantly upregulated in SA925 compared with in SA1088 and that downregulation of the *sigB* operon in SA1088 in response to H_2O_2 coincides with increased *agr* expression. Previously, it has been shown that RsbU inhibits *agr* expression.[58] Our findings that *agr* is expressed more highly in SA925 suggests that excess compensatory RsbU is strongly downregulating *agr* expression in SA1088. Perhaps because the expression of the *agr* system was upregulated in SA925, phenol-soluble modulins (PSMs) were dramatically upregulated in SA925 compared with in SA1088. This difference between SA925 and SA1088 may contribute to the enhanced survival of SA925 in human neutrophils, as PSMs have been shown to lyse neutrophils after phagocytosis, permitting *S. aureus* to escape.[59] However, the significantly reduced survival of JE2-crtN::Tn in neutrophils and under H_2O_2 stress compared with JE2 also suggests a direct role for staphyloxanthin (Figure 4).

We found preliminary evidence that staphyloxanthin may stimulate neutrophil recruitment in wounded tissues (Figures 4C–4F). Early neutrophil recruitment and activation are disrupted in diabetic wounds, though inflammation via neutrophils and macrophages has also been demonstrated to persist longer in diabetic compared with non-diabetic wounds, leading to a prolonged inflammatory phase.[60–62] Increased recruitment of neutrophils, simultaneous with protection from ROS, could enable high-staphyloxanthin strains of *S. aureus* to delay healing by facilitating inflammation without being cleared by the influx of neutrophils.

Our genomic analyses of DFU141's isolates indicated that SA1088's low-staphyloxanthin-associated *rsbU* mutation likely arose over time in DFU141 (Figure 5A). We identified 5 additional DFUs with possible intrahost, loss-of-function mutations in the sigB operon that were acquired during the DFU time course. Among non-healing DFUs, staphyloxanthin production was lower in isolates collected at later observation weeks on average (Figure 6B). These findings suggest a more nuanced relationship between staphyloxanthin and *S. aureus* survival in DFUs: staphyloxanthin and other *sigB*-dependent phenotypes may be essential for establishing an infection after wounding but become less important, and possibly detrimental, during late-stage infection. This model, though counterintuitive, would be consistent with observations in other *S. aureus* infection contexts. For example, Entenza et al. found that a clinical strain of *S. aureus* that overproduced sigB yielded much higher CFU counts than other strains 16 h following infection in a murine endocarditis model but much lower CFU counts 72 h post-infection.[39] Long et al. found evidence that *rsbU* is under selection for loss-of-function mutations as *S. aureus* infections in cystic fibrosis airways transition from acute to chronic.[56] Therefore, though staphyloxanthin confers resistance neutrophils and contributes to delayed DFU healing, its benefits to *S. aureus* in the wound environment may be specific to early-stage infection rather than late-stage chronic persistence.

In this study, we have identified staphyloxanthin as an *S. aureus* phenotype contributing to delayed healing in DFUs. We show that staphyloxanthin delays diabetic wound healing in a murine model. *In vitro*, staphyloxanthin increased *S. aureus* survival from oxidative stress and neutrophil engulfment, as demonstrated using both clinical and lab strain/transposon mutant strain comparisons. Novel strategies to manage and treat DFUs, especially those with low risk of further promoting anti-microbial resistance, are urgently needed. Our study puts forth staphyloxanthin as a promising early-stage treatment target for DFUs colonized or infected with *S. aureus*.

LIMITATIONS OF THE STUDY

In the clinical isolate SA1088, we attribute the low-staphyloxanthin phenotype to a mutation in a gene (*rsbU*) within the stress-responsive sigB operon. Though overall these isolates were remarkably similar at the genome level aside from this mutation, isolate SA925 contained a ϕSa3mw phage insertion that was absent in SA1088. Without direct complementation of *rsbU* or the introduction of an *rsbU* mutant, within these clinical isolates, we cannot attribute delayed healing associated with SA925 vs. SA1088 solely to differences in staphyloxanthin production. Furthermore, though staphyloxanthin delayed healing in murine diabetic wounds and conferred a clear survival advantage to *S. aureus* against neutrophils and ROS *in vitro*, we did not observe a difference in *S. aureus* CFUs recovered from wounds treated with JE2 compared with staphyloxanthin-deficient JE2-crtN::Tn. We did, however, recover significantly more *S. aureus* from SA925-than SA1088-treated wounds at days 3 and 7, suggesting a strong difference in survival between these strains *in vivo* (Figure S3). Because SA925 contained a ϕSa3mw phage insertion that was absent in SA1088, it is possible that elements on this phage may be contributing to this effect. Finally, a limitation of the longitudinal analysis of staphyloxanthin production across patient time courses is that the DFUs were of variable duration at time of enrollment, and we could not define when *S. aureus* was originally introduced to the wound.

STAR★METHODS

RESOURCE AVAILABILITY

Lead contact—Further information and requests for resources and reagents should be directed to and will be fulfilled by the lead contact and corresponding author, Elizabeth Grice (egrice@pennmedicine.upenn.edu).

Materials availability—All unique/stable reagents generated in this study are available from the Lead Contact with a complete Materials Transfer Agreement.

Data and code availability

- Genomic and transcriptomic data are deposited in NCBI under Bioproject PRJNA1015705.
- Custom code used is available at https://github.com/Grice-Lab/Staphyloxanthin (https://doi.org/10.5281/zenodo.8383736)

- Any additional information required to reanalyze the data reported in this work is available from the lead contact upon request.

EXPERIMENTAL MODEL AND STUDY PARTICIPANT DETAILS

Animal models and husbandry conditions—All mouse experiments were conducted under protocols approved by the University of Pennsylvania Institutional Animal Care and Use Committee (Protocol 804065). All mice were housed and maintained in an ABSL II and specific pathogen free facility in the Clinical Research Building vivarium at the University of Pennsylvania. The following strains of mice were used in these studies: C57BL6/J (JAX stock #000664) and B6.BKS(D)-*Lepr*^{db}/J (JAX stock #000697).[38]

Excisional wound model: Both male (n = 24) and female (n = 33) mice were used and housed individually during 3 independent experiments. Dorsal region was shaved when mice were 12 weeks old. Two full thickness excisional wounds of 8mm were created by punch Biopsy tool (Miltek) on shaved dorsal skin. Wounds were inoculated wtih 2×10^8 CFU of *S. aureus* or PBS with 10% glycerol vehicle control and the wound covered with transparent film (Tegaderm, 3M). Each wound was photographed and measured at the time of wounding (t = 0), day 3, day 7 and day 14. For experiment #3 with males, wounds were also photographed and measured at day 21. After day 7, the transparent film was removed. All experimental procedures were conducted on mice anesthetized with isoflurane and Bupivacaine (0.1 mg) and Bupinorphine-SR (0.05mg) were administered for pain relief. Mice were administered Diet Gel Recovery (Clear H2O) every 3 days to prevent weight loss. Wound measurements were made in ImageJ and represent the mean of 3 independent measurements. Wilcoxon sum rank tests were performed to compare groups. CFUs from experiment #3 were calculated from suspensions of 12mm punch biopsies from day 21 wounds. For day 3 and 7 CFU measures, this process was repeated on 4 female mice per group and experiments were ended at the time of biopsy collection and CFU plating.

Ear punch wound model: Female 8 week old C57BL/6 or db/db mice were ear-punched using a 2 mm Animal Ear-Punch (Fisher Scientific) and 1×10^8 CFU of bacteria topically applied to the entire mouse using sterile cotton swabs at Day 0 and Day 4 post ear-punch. At Day 7 post ear-punch, pictures of the punch were taken for calculation of wound area and a digital caliper (Model PK-0505, Mitutoyo) was used to measure ear thickness. Ear tissue was collected for flow cytometry to assess neutrophil recruitment.

Human blood and neutrophils—Primary human neutrophils and whole blood were freshly drawn from healthy human subjects according to a protocol approved by the University of Pennsylvania Institutional Review Board #851659. Both male and female subjects between ages 28 and 61 were used. Three individuals were used in each experiment. Gender, race, ethnicity, and socioeconomic status are not available for participants.

Microbial strains

***DFU100* S. aureus *strains*:** The DFU100 subjects that strains were collected from are described in detail in previous publications.[14,71] The Institutional Review Boards at the University of Iowa (IRB#200706724) and the University of Pennsylvania approved the study

procedures (IRB#815195). Informed consent was obtained from all participants in writing. Subjects were 28–78 years of age (mean age 53 ± 9 years of age) and 26% were female. All subjects were confirmed diabetic (type I or II) and antibiotic naive at the beginning of the study, but maintained other medication regimens not related to their DFU. Information regarding race, gender, ancestry, and socioeconomic status were not used in this study. As previously described in Gardner et al. 2014, swab specimens were collected from 100 DFU during the course of a prospective cohort study of wound bioburden and clinical outcomes. Swabs were collected using the Levine technique to sample deep tissue fluid.[72] The swabs were placed in charcoal transport media and transported to the microbiology laboratory, where they were then vortexed in 1 mL of tryptic soy broth prior to dilution and plating. *S. aureus* was identified on Columbia blood agar (Remel) as yellow beta-hemolytic colonies that stained as Gram-positive cocci and tested catalase positive as well as *Staphylococcus* latex-agglutination positive. Unique isolates were banked as glycerol stocks and stored at −80C.

***Reference* S. aureus *strains*:** We used the following laboratory reference strains: *S. aureus* strains SA113 (ATCC #35556), 502A (ATCC #27217), JE2. The following reagents were provided by the Network on Antimicrobial Resistance in Staphylococcus aureus (NARSA) for distribution by BEI Resources, NIAID, NIH: *Staphylococcus* aureus subsp. aureus, Strain JE2,[73] NR-46543, and the corresponding transposon mutants:

NE382 (SAUSA300_2498), NR-46925.

NE1607 (SAUSA300_2025), NR-48149.

NE1109 (SAUSA300_2022), NR-47652.

NE1472 (SAUSA300_2023), NR-48014.

NE1872(SAUSA300_2024), NR-48414.

METHOD DETAILS

***In vitro* biofilm formation—**Clear 96-well plates were coated with bovine fibronectin (Millipore Sigma) by diluting 1 mg/mL bovine fibronectin solution into PBS to a final concentration of 25 μg/mL and adding 60 μL per well, then incubating coated plates for 1 h at 37°C. Excess fibronectin was removed by aspiration and plates washed 2 times with PBS. Overnight cultures of *S. aureus* were grown in trypticase soy broth (TSB) from single colonies and then diluted 1/100 in TSB with 5% dextrose and arrayed in technical triplicate. Each plate was then grown statically at 37°C for 24 h to allow biofilm matrix to form. Bacterial growth was visualized by plate reader at OD_{600} nm. The media was removed and the plate was gently washed by dipping it in distilled water. The biofilm was stained with 125 μL of 0.5% crystal violet solution (Millipore Sigma) in water and the plate was incubated for 5 min. 200uL of acetic acid was added to each well to solubilize crystal violet and pipetted to mix, then quantified on a Biotek Synergy HT plate reader at 570 nm. Three biological replicates were performed for each isolate. For normalization, each biofilm was compared to production from *S. aureus* SA113 grown on the same plate. Percent biofilm

production was calculated by dividing mean Abs_{570}/OD_{600} readings for each isolate and comparing to SA113 biofilm production.

Staphyloxanthin production—Cultures of each *S. aureus* isolate were grown in 5 mL TSB shaking at 37°C for 24 h from single colonies. Overnight growth was quantified on a Biotek Synergy HT plate reader at 600nm. Cultures were centrifuged for 1 min at 13,000 RPM and supernatant was removed. Each pellet was resuspended in 700 μL of methanol and incubated at 55°C for 10 min. Tubes were centrifuged for 2 min at 13,000 RPM. 300 μL from each tube was added to each well of a clear 96-well plate in triplicate and then quantified at Abs_{450} nm on a Biotek Synergy HT plate reader. Three biological replicates were performed for each isolate. For normalization, all isolates were compared to staphyloxanthin production from *S. aureus* 502A strain on the same plate. Percent staphyloxanthin production was calculated by dividing mean Abs_{450}/OD_{600} readings for each isolate and comparing to mean 502A staphyloxanthin production.

Staphylokinase activity—Overnight cultures of each *S. aureus* isolate were grown in TSB shaking at 37°C from single colonies. An aliquot of each culture (100 μL) was diluted 1:1 in PBS and OD_{600} was quantified on a Biotek Synergy HT plate reader. Simultaneously 1 mL was removed from each culture and centrifuged at 13,000 RPM for 1 min. Three 100mL aliquots of supernatant were removed to 3 wells on a clear 96-well plate. To the supernatants, 50 μL of human glu-plasminogen (0.04 mg/mL; Invitrogen) in Tris-buffered saline was added to each well and mixed by pipetting. The plate was incubated for 15 min at 37°C, followed by the addition of 20 μL plasmin specific chromogenic substrate S-2251(H-D-Val-Leu-Lys-paranitroanilide, 2 mmol/L, Chromogenix) to each well. Color was allowed to develop for 3 h at 37°C then measured at Abs_{405} on a plate reader. Color was compared to a standard curve of the output for purified staphylokinase diluted 2x from 2μg to 0.0625 μg.

Siderophore production—Using a protocol adapted from Schwyn et al. (1987),[29] overnight cultures of each *S. aureus* isolate were grown from single colonies in TSB with shaking at 37°C. An aliquot of 100 ¼L from each culture was diluted 1:1 with PBS and OD_{600} was quantified on a Biotek Synergy HT plate reader. One OD_{600} of cells was removed from each culture to an Eppendorf tube and centrifuged at 13,000 rpm for 1 min. Supernatant was removed and cells were resuspended in 1mL of PBS and incubated at 37°C for 48 h. Shuttle solution was added to previously described chrome azurol S (CAS) solution. Bacterial tubes were centrifuged for 1 min at 13,000 rpm. An aliquot of 500 μL of supernatant from each tube was added to a pre-prepared Eppendorf tube containing 1mL of CAS solution. Tubes were incubated for 2 h at room temperature in the dark. An aliquot of 300 μL from each tube was added to a clear 96 well plate in triplicate. Siderophore production was quantified on a plate reader at Abs_{630} and normalized as a percentage of Abs_{630}-measured color lost as compared to a Abs_{630} of a CAS blank. Three biological replicates were performed for each isolate.

Hydrogen peroxide survival assays in SA1088, SA925, JE2, and JE2-crtN::Tn —Cultures of *S. aureus* were grown in TSB overnight from single colonies. 500 μL of each

culture was centrifuged at 13000 rpm for 1 min. Supernatant was removed and cellular pellet was resuspended in 1 mL of PBS. 450 μL from each resuspended culture was aliquoted into two Eppendorf tubes. To one aliquot, an additional 450 μL of PBS was added. To the second aliquot, 450 μL diluted hydrogen peroxide was added. To dilute the hydrogen peroxide, 2 mL of stabilized 30% H_2O_2 (Sigma Thermo-Fisher) was added to 7 mL of water and mixed. The cultures were incubated for 2 h at 37°C then plated onto blood agar plates to quantify CFUs. Survival was calculated by comparing the plates with and without H_2O_2 for each culture.

Complementation of *S. aureus* JE2-crtN::Tn—Primers 20221121A (5′ CAGGAATTCAATGGCATTTCAATATAGGAG) and 20221121B (5′ ATCGGGATCCCTCACATCTTTCTCTTAGAC) were used to amplify the CrtM and CrtN genes from *S. aureus* JE2. The primers are identical to those designed by Liu et al. (2005), but with restriction sites EcoRI and BamHI replacing XbaI and BglII, respectively.[27] The PCR product was cloned into the xylose inducible expression plasmid pEPSA5.[35] Plasmid construction was confirmed by Oxford Nanopore sequencing (Plamidsaurus, Eugene, OR). The resulting plasmid, pEP-CrtMN, was passaged through *E. coli* IM08.[36] and then electroporated into *S. aureus* JE2-crtN::Tn with selection on TSA +35 μg/mL chloramphenicol. Restoration of staphyloxanthin production was observed by the appearance of a gold coloration in the pEP-CrtMN transformed JE2-crtN::Tn mutant colonies compared to the pale color of the control, pEPSA5, transformed colonies. The presence of complementing and control plasmids in the transformed strains was confirmed by colony PCR of transformants using primers 20230113A (ACACAATTTAACCCAGACGCT), 20230113B (GAGAC CCCACACTACCATCG), and 20230119A (TCGGCGTCAATACTTCACCT). We observed that on TSA and in TSB media there was high basal expression from the XylR promoter.

Hydrogen peroxide survival assays in crtMN-complemented JE2 mutant —Cultures of JE2(background strain), JE2-crtN::Tn/pEPSA5(transposon mutant with empty plasmid vector), and JE2-crtN::Tn/pEPcrtMN (transposon mutant with crtMN complementation) were grown in TSB with orbital shaking at 37°C for 48 h. JE2-crtN::Tn strains were selected with 10%(35μg/mL) chloramphenicol, and a volume of each culture containing 1.5×10^9 CFU was transferred in duplicates to a Falcon 14mL tube and taken to 500 μL with dPBS. A 0.30% hydrogen peroxide solution was prepared by combining 40μL stabilized 30% H_2O_2 with 3960μL dPBS. 500 μL of the diluted hydrogen peroxide or 500μL dPBS was then added to each Falcon tube containing a culture. The six Falcon tubes were then incubated at room temperature for 30 min, followed by 4°C in the dark for 45 min. Cultures were then plated onto tryptic soy agar plates for CFU counts. Survival was calculated as percent ratio of CFUs from H_2O_2-treated to those of the same culture treated with dPBS alone. This was repeated to achieve 4 replicates in total, and paired T-tests were performed on comparisons between strains within the same experimental replicate.

Polymyxin B survival assay—Cultures of *S. aureus* were grown in TSB overnight from single colonies. An aliquot of 200 μL of each culture was diluted 10x into 1x PBS and then split into two separate tubes. To one tube, 10 μL of 100 mM polymyxin B in ethanol was

added. To the other tube 10 μL of ethanol was added. Tubes were incubated at 37°C for 30 min with shaking and then each tube was plated on blood agar and CFUs quantified to compare survival with and without polymyxin.

Antibodies and flow cytometry—Single cell suspensions from the ear were obtained by using tweezers to separate the dorsal and ventral sides of the mouse ear and placing the sheets dorsal-side down in a 24 well plate with 1 mL/well of RPMI1640 containing 0.25 mg/mL of Liberase TL (Roche, Diagnostics Corp.) and 10 μg/mL of DNase I (Sigma-Aldrich). Sheets were incubated for 90 min at 37°C and a single cell suspension was obtained by dissociation using the plunger of a 3 mL syringe to break up the tissue on a 40 μm cell strainer (Falcon). Dissociated tissue was washed into a 50 mL conical using PBS containing 0.05% BSA and 20 μM EDTA. Staining for surface markers was performed by incubating the cells in single cell suspension with anti-mouse CD16/CD32 mouse Fc block (Thermo Fisher Scientific, RRID: AB_467135) and 10% rat-IgG in PBS. Dead cells were stained using LIVE/DEAD Fixable Aqua Dead Cell Stain Kit (Thermo Fisher Scientific, L34957) and surface markers were stained using CD45 (Clone: 30-F11, BioLegend, Cat 103108), CD8b (clone: YTS156.7.7, BioLegend, Cat 126609), CD11b (clone: M1/70, BioLegend, cat 101235), CD90.2 (clone: 30-H12, BioLegend, cat 105343), Ly6C (clone: HK1.4, BioLegend, cat 128041), Ly6G (clone: 18A, BioLegend, cat 127614), γδ TCR (clone: GL3, BioLegend, cat 118136), F4/80 (clone: t45–2342, BD Pharmigen, cat 565410), CD4 (Thermo Fisher Scientific, cat MCD0417), and CD11c (clone: N418, BioLegend, cat 117318). Cells were fixed using 2% formaldehyde and the data was collected using the LSR Fortessa flow cytometer (BD) and analyzed using FlowJo Software (BD).

Whole blood survival assay—Freshly drawn whole human blood (25 mL) was mixed with 1×10^4 *S aureus* and incubated with shaking for 4 h at 37°C. Samples were plated on blood agar and CFU quantified.

Neutrophil survival assay—Primary human neutrophils were isolated from freshly drawn human blood using Neutrophil Isolation Medium. Remnant red blood cells were removed from neutrophil pellet using RBC lysis buffer. *S. aureus* (4.5×10^6 CFU) was pre-incubated with 10% human serum for 15 min, washed with PBS, added to 3×10^5 neutrophils, and incubated at 37°C for 30 min. Gentamicin (400 μg/mL) was added to each tube to kill extracellular *S. aureus*. Pelleted neutrophils were washed with PBS then lysed with water (pH = 11.0). Neutrophil lysates were plated onto blood agar and bacterial CFUs were counted.

Whole genome sequencing—All DNA extractions were performed on overnight cultures of DFU141 isolates grown in 5 mL TSB from single colonies. Genomic DNA extractions for short read sequencing were prepared using the *Quick*-DNA Miniprep Plus Kit (Zymo Research). High molecular weight genomic DNA extractions were prepared using the Monarch HMW DNA Extraction Kit for Tissue (NEB). All 14 isolates cultured from DFU141 were initially sequenced with paired-end sequencing on Illumina HiSeq 2500 at PennCHOP Microbiome Core. SA929 and SA882 were resequenced on NextSeq 2000 at the Microbial Genome Sequencing Center (MiGS) due to suspected contamination (see

Whole Genome Assembly & Quality Control). All 14 isolates except SA929 were further sequenced using Oxford Nanopore long read sequencing at MiGS.

Whole genome assembly, processing, and quality control—Raw, demultiplexed short reads were trimmed using TrimGalore based on the output of FastQC.[68,74] Long reads were trimmed using Porechop.[64] Hybrid assembly was performed on the Illumina & Oxford Nanopore-sequenced isolates using Unicycler with default "Normal" settings for hybrid assembly and Illumina short read-only assembly, respectively.[63] Contigs <100 bp in length were removed, and we performed Mash screens against each assembled genome to confirm its identity as *Staphylococcus aureus*.[66] To check for intra-species contamination in the short reads, trimmed short reads from each isolate were mapped to a SPAdes *de novo* assembly for that isolate and SNP-called using Bowtie2 and Samtools, respectively.[75,76] Based on Raven et al.'s 2020 benchmarking study in clinical MRSA sequences, we counted the number of SNPs in each alignment with ≥10X depth located at least 50 bp apart from one another, and considered assemblies contaminated if they contained >30 such SNPs.[77] To check for contamination in hybrid genome assemblies, we performed HMM searches for Anvio's set of bacterial universal single copy genes (USCGs) in each assembled genome and screened genomes for multiple copies of theoretically single copy genes.[67,77]

Phylogeny estimation—PubMLST assigned each of the 14 *S aureus* isolates from DFU141 to Clonal Complex 1 (CC1). We therefore estimated a maximum likelihood phylogeny from the 14 *S aureus* genomes from DFU141 along with a CC1 MW2 strain reference genome outgroup (NCBI accession *GCF_000011265.1*). We annotated CDS loci in each genome assembly using Prokka, and performed a probabilistic multiple alignment of shared (core) genes using Roary and PRANK.[44,78] A maximum likelihood phylogeny was estimated from the core gene alignment using RaxML's GTRGAMMA model with 100 random starts.[65]

Genomic analysis of DFU141 staphyloxanthin mutants—To identify variants consistently and uniquely found in the three low staphyloxanthin-producing genomes from DFU141 as compared to the 11 high-staphyloxanthin-producing genomes, we first annotated 43 genomic differences between SA925 (high) and SA1088 (low) using NucDiff.[45] We then annotated the presence/absence of each of these 43 variants in comparisons of SA925 to each of the other 12 genomes from DFU141, identifying 4 variants total which were consistently found in comparisons of SA925 to all three low-staphyloxanthin isolates, but none of the high-staphyloxanthin isolates. We further characterized each of these 4 variants by their genomic position relative to predicted coding regions in annotations by both Prokka and PGAP.[63] For variants predicted to be in coding regions, we performed BLAST alignments of predicted amino acid sequences for the CDS containing each variant from SA925 and SA1088.

Comparisons between amino acid sequences in sigma B operon genes—We classified *S. aureus* whole genomes into clonal complexes (CCs) using PubMLST.[42] We made multi-fasta files of sequences for each of *rsbU*, *rsbW*, *rsbV*, and *sigB*, using translated amino acid sequences generated for all CDS by PGAP. We then used a custom python script

to compare all 220 genomes' amino acid sequences for each component to that of the parent strain for JE2 (GCA_000013465.1). For each DFU, we identified any amino acid sequence variants that were present in at least one, but not all, isolates from that DFU belonging to a single CC. We plotted the staphyloxanthin measures taken for Figure 1 for isolates in the DFU/CC grouping with the variant versus those without (Figure 6A).

Bacterial RNA sequencing—Cultures of SA925 and SA1088 (5 mL) were grown overnight in TSB from single colonies. Samples were back diluted 1/1000 and grown with and without 1% H_2O_2 shaking at 37°C to an OD 600 of 1.0. RNA was extracted from each sample by resuspending each bacterial pellet in 1 mL TriZol and homogenizing in a BioSpec MiniBeadbeater 16 with 0.1 mm zirconium particles (BioSpec) followed by centrifuging lysate at 14,000 g for 3 min. Following centrifugation, supernatant was mixed with .5mL 95% ethanol and treated using the Direct-zol RNA Miniprep Plus Kit (Zymo Research) and treated with DNAse 1. RNA integrity was assessed with a 2100 Bioanalyzer and the Prokaryote Total RNA 6000 Pico Kit (Agilent). All samples had an RNA Integrity Number (RIN) > 8. RNA concentration was quantified on Qubit using the RNA Broad Range assay (Invitrogen). Ribosomal RNA was depleted and libraries were constructed using the Illumina Stranded Total RNA Prep with Ribo-Zero Plus (Illumina) using 100 ng of RNA input. IDT for Illumina UD indexes were ligated to the libraries. Library quality control was performed with the Agilent DNA 1000 kit on the Bioanalyzer. The concentration of the libraries was quantified using the Qubit dsDNA high sensitivity assay. Libraries were pooled in equimolar amounts, denatured, and diluted to a final concentration of 1.5 p.m. Libraries were then sequenced on the NextSeq 500 using the mid-output kit, generating 75-bp paired-end reads. Transcriptomic sequencing results represent three biological replicates with the exception of SA925 under H_2O_2 conditions, which represents two replicates due to one replicate failing to yield adequate reads for analysis.

Transcriptomic analysis of SA1088 and SA925—Demultiplexed reads were merged within replicates and checked for quality using FastQC on forward and reverse reads separately. Reads were trimmed using the *Trim Galore!* wrapper for FastQC and CutAdapt.[68] Trimmed reads were aligned to the complete SA925 genome using Bowtie2 and sorted using *Samtools*. Read counts per-gene were obtained with *featureCounts()* from the *Rsubread* package, using CDS features from an SA925 genome annotation file reformatted from the output of the PGAP docker image (ncbi/pgap:2021–11-29.build5742).[70] We mapped PGAP-annotated RefSeq IDs for each CDS to UniProt to obtain gene names and GO terms. Differential expression analysis between treatments and strains were performed using DESeq2, and plots in Figure 5 were produced using *ggplot2* and, with functional categories for stress response and toxicity assigned to genes via a combination of QuickGO and UniProt mappings and manual annotation based on Gaupp et al.'s 2012 review article.[71–81]

QUANTIFICATION AND STATISTICAL ANALYSIS

Figures were generated in R. Deduplication and hypothesis testing methods used, along with sample size, and measures of dispersion (where applicable) are reported in figure legends. We defined statistical significance at alpha = 0.05. For Figure 1 and S1 hypothesis testing,

isolates were deduplicated by individual DFU using the methods indicated in figure titles and legends using the *dplyr* package and base R's mean(), median(), and max() commands. For linear mixed model estimates of effect of healing outcome on isolate phenotypes, phenotype measures were min-max normalized, then fit to models of (Phenotype ~ (1| patient) + HealingOutcome) using *lme4*, and model fits are reported in Table S3.[31]

Supplementary Material

Refer to Web version on PubMed Central for supplementary material.

ACKNOWLEDGMENTS

We thank Ms. Jamie Pan and Ms. Anisa Ray for their assistance with phlebotomy and Dr. Daniel Shin, Associate Director of the Data Science and Informatics Core of the Penn SBDRC, for statistical consultation. The following reagent was provided by the Network on Antimicrobial Resistance in Staphylococcus aureus (NARSA) for distribution by BEI Resources, NIAID, NIH: Staphylococcus aureus subsp. aureus, Strain JE2, Transposon Mutant NE382 (SAUSA300_2498), NR-46925. We thank current and former members of the Grice lab and the Department of Dermatology for critical discussions and review of the work. This work was funded by the following grants from the NIH, NINR (R01NR015639 to E.A.G. and R01NR009448 to S.E.G.); the NIAID (R01AI137526 to P.J.P. and R01AI143790 to E.A.G.); the NIAMS (F31AR079901 to V.M.L., F31AR079852 to E.K.W., K99AR081404 to A.U., and T32AR007465 to A.R.M.-V.); the NIDDK Diabetic Complications Consortium (grant DK076169 to E.A.G.); the Burroughs Wellcome Fund PATH Award; and the Dermatology Foundation Sun Pharma Research Award. Additional sources of support include the UPenn Blavatnik Family Fellowship (A.E.C.), the Prevent Cancer Foundation Awesome Games Done Quick fellowship (A.U.), and the Penn SBDRC (supported by NIH/NIAMS P30AR069589). The sampling scheme illustration in Figure 1A was created with Biorender.com.

INCLUSION AND DIVERSITY

We support inclusive, diverse, and equitable conduct of research.

REFERENCES

1. Armstrong DG, Boulton AJM, and Bus SA (2017). Diabetic Foot Ulcers and Their Recurrence. N. Engl. J. Med 376, 2367–2375. 10.1056/NEJMra1615439. [PubMed: 28614678]
2. Everett E, and Mathioudakis N. (2018). Update on management of diabetic foot ulcers. Ann. N. Y. Acad. Sci 1411, 153–165. 10.1111/nyas.13569. [PubMed: 29377202]
3. Hartemann-Heurtier A, and Senneville E. (2008). Diabetic foot osteomyelitis. Diabetes Metab. 34, 87–95. 10.1016/j.diabet.2007.09.005. [PubMed: 18242114]
4. Hoffstad O, Mitra N, Walsh J, and Margolis DJ (2015). Diabetes, lower-extremity amputation, and death. Diabetes Care 38, 1852–1857. 10.2337/dc15-0536. [PubMed: 26203063]
5. Martins-Mendes D, Monteiro-Soares M, Boyko EJ, Ribeiro M, Barata P, Lima J, and Soares R. (2014). The independent contribution of diabetic foot ulcer on lower extremity amputation and mortality risk. J. Diabetes Complications 28, 632–638. 10.1016/j.jdiacomp.2014.04.011. [PubMed: 24877985]
6. Armstrong DG, Wrobel J, and Robbins JM (2007). Guest Editorial: are diabetes-related wounds and amputations worse than cancer? Int. Wound J 4, 286–287. 10.1111/j.1742-481X.2007.00392.x. [PubMed: 18154621]
7. Moulik PK, Mtonga R, and Gill GV (2003). Amputation and mortality in new-onset diabetic foot ulcers stratified by etiology. Diabetes Care 26, 491–494. 10.2337/diacare.26.2.491. [PubMed: 12547887]
8. Dunyach-Remy C, Ngba Essebe C, Sotto A, and Lavigne J-P (2016). Staphylococcus aureus Toxins and Diabetic Foot Ulcers: Role in Pathogenesis and Interest in Diagnosis. Toxins 8, E209. 10.3390/toxins8070209.

9. Gardiner M, Vicaretti M, Sparks J, Bansal S, Bush S, Liu M, Darling A, Harry E, and Burke CM (2017). A longitudinal study of the diabetic skin and wound microbiome. PeerJ 5, e3543. 10.7717/peerj.3543.
10. Citron DM, Goldstein EJC, Merriam CV, Lipsky BA, and Abramson MA (2007). Bacteriology of moderate-to-severe diabetic foot infections and in vitro activity of antimicrobial agents. J. Clin. Microbiol 45, 2819–2828. 10.1128/JCM.00551-07. [PubMed: 17609322]
11. Sloan TJ, Turton JC, Tyson J, Musgrove A, Fleming VM, Lister MM, Loose MW, Sockett RE, Diggle M, Game FL, and Jeffcoate W. (2019). Examining diabetic heel ulcers through an ecological lens: microbial community dynamics associated with healing and infection. J. Med. Microbiol 68, 230–240. 10.1099/jmm.0.000907. [PubMed: 30624175]
12. Tong SYC, Davis JS, Eichenberger E, Holland TL, and Fowler VG (2015). Staphylococcus aureus infections: epidemiology, pathophysiology, clinical manifestations, and management. Clin. Microbiol. Rev 28, 603–661. 10.1128/CMR.00134-14. [PubMed: 26016486]
13. Wolcott RD, Hanson JD, Rees EJ, Koenig LD, Phillips CD, Wolcott RA, Cox SB, and White JS (2016). Analysis of the chronic wound microbiota of 2,963 patients by 16S rDNA pyrosequencing. Wound Repair Regen. 24, 163–174. 10.1111/wrr.12370. [PubMed: 26463872]
14. Gardner SE, Haleem A, Jao Y-L, Hillis SL, Femino JE, Phisitkul P, Heilmann KP, Lehman SM, and Franciscus CL (2014). Cultures of diabetic foot ulcers without clinical signs of infection do not predict outcomes. Diabetes Care 37, 2693–2701. 10.2337/dc14-0051. [PubMed: 25011945]
15. Olaniyi R, Pozzi C, Grimaldi L, and Bagnoli F. (2017). Staphylococcus aureus-Associated Skin and Soft Tissue Infections: Anatomical Localization, Epidemiology, Therapy and Potential Prophylaxis. Curr. Top. Microbiol. Immunol 409, 199–227. 10.1007/82_2016_32. [PubMed: 27744506]
16. Sotto A, Lina G, Richard J-L, Combescure C, Bourg G, Vidal L, Jourdan N, Etienne J, and Lavigne J-P (2008). Virulence potential of Staphylococcus aureus strains isolated from diabetic foot ulcers: a new paradigm. Diabetes Care 31, 2318–2324. 10.2337/dc08-1010. [PubMed: 18809632]
17. Sotto A, Richard J-L, Messad N, Molinari N, Jourdan N, Schuldiner S, Sultan A, Carrière C, Canivet B, Landraud L, et al. (2012). Distinguishing colonization from infection with Staphylococcus aureus in diabetic foot ulcers with miniaturized oligonucleotide arrays: a French multicenter study. Diabetes Care 35, 617–623. 10.2337/dc11-1352. [PubMed: 22301121]
18. Kalan LR, Meisel JS, Loesche MA, Horwinski J, Soaita I, Chen X, Uberoi A, Gardner SE, and Grice EA (2019). Strain- and Species-Level Variation in the Microbiome of Diabetic Wounds Is Associated with Clinical Outcomes and Therapeutic Efficacy. Cell Host Microbe 25, 641– 655.e5. 10.1016/j.chom.2019.03.006.
19. Roy S, Elgharably H, Sinha M, Ganesh K, Chaney S, Mann E, Miller C, Khanna S, Bergdall VK, Powell HM, et al. (2014). Mixed-species biofilm compromises wound healing by disrupting epidermal barrier function. J. Pathol 233, 331–343. 10.1002/path.4360. [PubMed: 24771509]
20. Schierle CF, De la Garza M, Mustoe TA, and Galiano RD (2009). Staphylococcal biofilms impair wound healing by delaying reepithelialization in a murine cutaneous wound model. Wound Repair Regen. 17, 354–359. 10.1111/j.1524-475X.2009.00489.x. [PubMed: 19660043]
21. Dale SE, Doherty-Kirby A, Lajoie G, and Heinrichs DE (2004). Role of siderophore biosynthesis in virulence of Staphylococcus aureus: identification and characterization of genes involved in production of a siderophore. Infect. Immun 72, 29–37. 10.1128/IAI.72.1.29-37.2004. [PubMed: 14688077]
22. Harrison F, Paul J, Massey RC, and Buckling A. (2008). Interspecific competition and siderophore-mediated cooperation in Pseudomonas aeruginosa. ISME J. 2, 49–55. 10.1038/ismej.2007.96. [PubMed: 18180746]
23. Rooijakkers SHM, van Wamel WJB, Ruyken M, van Kessel KPM, and van Strijp J.a.G. (2005). Anti-opsonic properties of staphylokinase. Microbes Infect. 7, 476–484. 10.1016/j.micinf.2004.12.014. [PubMed: 15792635]
24. Cano Sanchez M, Lancel S, Boulanger E, and Neviere R. (2018). Targeting Oxidative Stress and Mitochondrial Dysfunction in the Treatment of Impaired Wound Healing: A Systematic Review. Antioxidants 7, E98. 10.3390/antiox7080098.

25. Dworzański J., Strycharz-Dudziak M, Kliszczewska E, Kie1czykowska M, Dworzańska A, Drop B, and Polz-Dacewicz M (2020). Glutathione peroxidase (GPx) and superoxide dismutase (SOD) activity in patients with diabetes mellitus type 2 infected with Epstein-Barr virus. PLoS One 15, e0230374. 10.1371/journal.pone.0230374.
26. Clauditz A, Resch A, Wieland K-P, Peschel A, and Gö tz F (2006). Staphyloxanthin plays a role in the fitness of Staphylococcus aureus and its ability to cope with oxidative stress. Infect. Immun 74, 4950–4953. 10.1128/IAI.00204-06. [PubMed: 16861688]
27. Liu GY, Essex A, Buchanan JT, Datta V, Hoffman HM, Bastian JF, Fierer J, and Nizet V. (2005). Staphylococcus aureus golden pigment impairs neutrophil killing and promotes virulence through its antioxidant activity. J. Exp. Med 202, 209–215. 10.1084/jem.20050846. [PubMed: 16009720]
28. O'Toole GA (2011). Microtiter Dish Biofilm Formation Assay. J. Vis. Exp 47.
29. Schwyn B, and Neilands JB (1987). Universal chemical assay for the detection and determination of siderophores. Anal. Biochem 160, 47–56. 10.1016/0003-2697(87)90612-9. [PubMed: 2952030]
30. Kwiecinski J, Jacobsson G, Karlsson M, Zhu X, Wang W, Bremell T, Josefsson E, and Jin T. (2013). Staphylokinase promotes the establishment of Staphylococcus aureus skin infections while decreasing disease severity. J. Infect. Dis 208, 990–999. 10.1093/infdis/jit288. [PubMed: 23801604]
31. Bates D, Mächler M, Bolker B, and Walker S. (2015). Fitting Linear Mixed-Effects Models Using lme4. J. Stat. Soft 67. 10.18637/jss.v067.i01.
32. Fey PD, Endres JL, Yajjala VK, Widhelm TJ, Boissy RJ, Bose JL, and Bayles KW (2013). A Genetic Resource for Rapid and Comprehensive Phenotype Screening of Nonessential Staphylococcus aureus Genes. mBio 4, e00537–e00512. 10.1128/mbio.00537-12.
33. Pelz A, Wieland K-P, Putzbach K, Hentschel P, Albert K, and Götz F. (2005). Structure and Biosynthesis of Staphyloxanthin from Staphylococcus aureus. J. Biol. Chem 280, 32493–32498. 10.1074/jbc.M505070200.
34. Valliammai A, Selvaraj A, Muthuramalingam P, Priya A, Ramesh M, and Pandian SK (2021). Staphyloxanthin inhibitory potential of thymol impairs antioxidant fitness, enhances neutrophil mediated killing and alters membrane fluidity of methicillin resistant Staphylococcus aureus. Biomed. Pharmacother 141, 111933. 10.1016/j.biopha.2021.111933.
35. Forsyth RA, Haselbeck RJ, Ohlsen KL, Yamamoto RT, Xu H, Trawick JD, Wall D, Wang L, Brown-Driver V, Froelich JM, et al. (2002). A genome-wide strategy for the identification of essential genes in Staphylococcus aureus. Mol. Microbiol 43, 1387–1400. 10.1046/j.1365-2958.2002.02832.x. [PubMed: 11952893]
36. Monk IR, Tree JJ, Howden BP, Stinear TP, and Foster TJ (2015). Complete Bypass of Restriction Systems for Major Staphylococcus aureus Lineages. mBio 6, e00308–e00315. 10.1128/mbio.00308-15.
37. Mishra NN, Liu GY, Yeaman MR, Nast CC, Proctor RA, McKinnell J, and Bayer AS (2011). Carotenoid-related alteration of cell membrane fluidity impacts Staphylococcus aureus susceptibility to host defense peptides. Antimicrob. Agents Chemother 55, 526–531. 10.1128/AAC.00680-10. [PubMed: 21115796]
38. Coleman DL (1978). Obese and diabetes: two mutant genes causing diabetes-obesity syndromes in mice. Diabetologia 14, 141–148. 10.1007/BF00429772. [PubMed: 350680]
39. Entenza J-M, Moreillon P, Senn MM, Kormanec J, Dunman PM, Berger-Bächi B, Projan S, and Bischoff M. (2005). Role of σB in the Expression of Staphylococcus aureus Cell Wall Adhesins ClfA and FnbA and Contribution to Infectivity in a Rat Model of Experimental Endocarditis. Infect. Immun 73, 990–998. 10.1128/iai.73.2.990-998.2005. [PubMed: 15664942]
40. Beavers WN, and Skaar EP (2016). Neutrophil-generated oxidative stress and protein damage in Staphylococcus aureus. Pathog. Dis 74, ftw060. 10.1093/femspd/ftw060.
41. Leung TH, Snyder ER, Liu Y, Wang J, and Kim SK (2015). A cellular, molecular, and pharmacological basis for appendage regeneration in mice. Genes Dev. 29, 2097–2107. 10.1101/gad.267724.115. [PubMed: 26494786]
42. Jolley KA, Bray JE, and Maiden MCJ (2018). Open-access bacterial population genomics: BIGSdb software, the PubMLST.org website and their applications. Wellcome Open Res. 3, 124. 10.12688/wellcomeopenres.14826.1. [PubMed: 30345391]

43. Seemann T. (2014). Prokka: rapid prokaryotic genome annotation. Bioinformatics 30, 2068–2069. 10.1093/bioinformatics/btu153. [PubMed: 24642063]
44. Page AJ, Cummins CA, Hunt M, Wong VK, Reuter S, Holden MTG, Fookes M, Falush D, Keane JA, and Parkhill J. (2015). Roary: rapid large-scale prokaryote pan genome analysis. Bioinformatics 31, 3691–3693. 10.1093/bioinformatics/btv421. [PubMed: 26198102]
45. Khelik K, Lagesen K, Sandve GK, Rognes T, and Nederbragt AJ (2017). NucDiff: in-depth characterization and annotation of differences between two sets of DNA sequences. BMC Bioinf. 18, 338. 10.1186/s12859-017-1748-z.
46. Haft DH, DiCuccio M, Badretdin A, Brover V, Chetvernin V, O'Neill K, Li W, Chitsaz F, Derbyshire MK, Gonzales NR, et al. (2018). Re-fSeq: an update on prokaryotic genome annotation and curation. Nucleic Acids Res. 46, D851–D860. 10.1093/nar/gkx1068. [PubMed: 29112715]
47. Palma M, and Cheung AL (2001). sigma(B) activity in Staphylococcus aureus is controlled by RsbU and an additional factor(s) during bacterial growth. Infect. Immun 69, 7858–7865. 10.1128/IAI.69.12.7858-7865.2001. [PubMed: 11705968]
48. Giachino P, Engelmann S, and Bischoff M. (2001). Sigma(B) activity depends on RsbU in Staphylococcus aureus. J. Bacteriol 183, 1843–1852. 10.1128/JB.183.6.1843-1852.2001. [PubMed: 11222581]
49. Baba T, Takeuchi F, Kuroda M, Yuzawa H, Aoki K.i., Oguchi A, Nagai Y, Iwama N, Asano K, Naimi T, et al. (2002). Genome and virulence determinants of high virulence community-acquired MRSA. Lancet 359, 1819–1827. 10.1016/s0140-6736(02)08713-5. [PubMed: 12044378]
50. Bischoff M, Dunman P, Kormanec J, Macapagal D, Murphy E, Mounts W, Berger-Bä chi B, and Projan S (2004). Microarray-Based Analysis of the Staphylococcus aureus σB Regulon. J. Bacteriol 186, 4085–4099. 10.1128/jb.186.13.4085-4099.2004. [PubMed: 15205410]
51. Palazzolo-Ballance AM, Reniere ML, Braughton KR, Sturdevant DE, Otto M, Kreiswirth BN, Skaar EP, and DeLeo FR (2008). Neutrophil microbicides induce a pathogen survival response in community-associated methicillin-resistant Staphylococcus aureus. J. Immunol 180, 500–509. 10.4049/jimmunol.180.1.500. [PubMed: 18097052]
52. Ramond E, Jamet A, Ding X, Euphrasie D, Bouvier C, Lallemant L, He X, Arbibe L, Coureuil M, and Charbit A. (2021). Reactive Oxygen Species-Dependent Innate Immune Mechanisms Control Methicillin-Resistant Staphylococcus aureus Virulence in the Drosophila Larval Model. mBio 12, e0027621. 10.1128/mBio.00276-21.
53. Olivier AC, Lemaire S, Van Bambeke F, Tulkens PM, and Oldfield E. (2009). Role of rsbU and staphyloxanthin in phagocytosis and intracellular growth of Staphylococcus aureus in human macrophages and endothelial cells. J. Infect. Dis 200, 1367–1370. 10.1086/606012. [PubMed: 19817587]
54. Stahlhut SG, Alqarzaee AA, Jensen C, Fisker NS, Pereira AR, Pinho MG, Thomas VC, and Frees D. (2017). The ClpXP protease is dispensable for degradation of unfolded proteins in Staphylococcus aureus. Sci. Rep 7, 11739. 10.1038/s41598-017-12122-y.
55. Wozniak DJ, Tiwari KB, Soufan R, and Jayaswal RK (2012). The mcsB gene of the clpC operon is required for stress tolerance and virulence in Staphylococcus aureus. Microbiology (Read.) 158, 2568–2576. 10.1099/mic.0.060749-0.
56. Long DR, Wolter DJ, Lee M, Precit M, McLean K, Holmes E, Penewit K, Waalkes A, Hoffman LR, and Salipante SJ (2021). Polyclonality, Shared Strains, and Convergent Evolution in Chronic Cystic Fibrosis Staphylococcus aureus Airway Infection. Am. J. Respir. Crit. Care Med 203, 1127–1137. 10.1164/rccm.202003-0735OC. [PubMed: 33296290]
57. Touati D. (2000). Iron and oxidative stress in bacteria. Arch. Biochem. Biophys 373, 1–6. 10.1006/abbi.1999.1518. [PubMed: 10620317]
58. Bischoff M, Entenza JM, and Giachino P. (2001). Influence of a functional sigB operon on the global regulators sar and agr in Staphylococcus aureus. J. Bacteriol 183, 5171–5179. 10.1128/JB.183.17.5171-5179.2001. [PubMed: 11489871]
59. Surewaard BGJ, de Haas CJC, Vervoort F, Rigby KM, DeLeo FR, Otto M, van Strijp J. a.G., and Nijland R (2013). Staphylococcal alpha-phenol soluble modulins contribute to neutrophil lysis after phagocytosis. Cell Microbiol. 15, 1427–1437. 10.1111/cmi.12130. [PubMed: 23470014]

60. Roy R, Zayas J, Singh SK, Delgado K, Wood SJ, Mohamed MF, Frausto DM, Albalawi YA, Price TP, Estupinian R, et al. (2022). Overriding impaired FPR chemotaxis signaling in diabetic neutrophil stimulates infection control in murine diabetic wound. Elife 11, e72071. 10.7554/eLife.72071.
61. Wetzler C, Kä mpfer H, Stallmeyer B, Pfeilschifter J, and Frank S (2000). Large and Sustained Induction of Chemokines during Impaired Wound Healing in the Genetically Diabetic Mouse: Prolonged Persistence of Neutrophils and Macrophages during the Late Phase of Repair. J. Invest. Dermatol 115, 245–253. 10.1046/j.1523-1747.2000.00029.x. [PubMed: 10951242]
62. Pierce GF (2001). Inflammation in Nonhealing Diabetic Wounds: The Space-Time Continuum Does Matter. Am. J. Pathol 159, 399–403. 10.1016/S0002-9440(10)61709-9. [PubMed: 11485896]
63. Wick RR, Judd LM, Gorrie CL, and Holt KE (2017). Unicycler: Resolving bacterial genome assemblies from short and long sequencing reads. PLoS Comput. Biol 13, e1005595. 10.1371/journal.pcbi.1005595.
64. Wick R. Porechop. (2023). https://github.com/rrwick/Porechop.
65. Stamatakis A. (2014). RAxML version 8: a tool for phylogenetic analysis and post-analysis of large phylogenies. Bioinformatics 30, 1312–1313. 10.1093/bioinformatics/btu033. [PubMed: 24451623]
66. Ondov BD, Treangen TJ, Melsted P, Mallonee AB, Bergman NH, Koren S, and Phillippy AM (2016). Mash: fast genome and metagenome distance estimation using MinHash. Genome Biol. 17, 132. 10.1186/s13059-016-0997-x. [PubMed: 27323842]
67. Eren AM, Kiefl E, Shaiber A, Veseli I, Miller SE, Schechter MS, Fink I, Pan JN, Yousef M, Fogarty EC, et al. (2021). Community-led, integrated, reproducible multi-omics with anvi'o. Nat. Microbiol 6, 3–6. 10.1038/s41564-020-00834-3. [PubMed: 33349678]
68. Krueger F. Trim Galore. (2023). https://github.com/FelixKrueger/TrimGalore
69. Love MI, Huber W, and Anders S. (2014). Moderated estimation of fold change and dispersion for RNA-seq data with DESeq2. Genome Biol. 15, 550. 10.1186/s13059-014-0550-8. [PubMed: 25516281]
70. Liao Y, Smyth GK, and Shi W. (2019). The R package Rsubread is easier, faster, cheaper and better for alignment and quantification of RNA sequencing reads. Nucleic Acids Res. 47, e47. 10.1093/nar/gkz114. [PubMed: 30783653]
71. Loesche M, Gardner SE, Kalan L, Horwinski J, Zheng Q, Hodkinson BP, Tyldsley AS, Franciscus CL, Hillis SL, Mehta S, et al. (2017). Temporal stability in chronic wound microbiota is associated with poor healing. J. Invest. Dermatol 137, 237–244. 10.1016/j.jid.2016.08.009. [PubMed: 27566400]
72. Gardner SE, Frantz RA, Saltzman CL, Hillis SL, Park H, and Scherubel M. (2006). Diagnostic validity of three swab techniques for identifying chronic wound infection. Wound Repair Regen. 14, 548–557. 10.1111/j.1743-6109.2006.00162.x. [PubMed: 17014666]
73. Paudel A, Panthee S, Hamamoto H, Grunert T, and Sekimizu K. (2021). YjbH regulates virulence genes expression and oxidative stress resistance in Staphylococcus aureus. Virulence 12, 470–480. 10.1080/21505594.2021.1875683. [PubMed: 33487122]
74. Andrews S. FastQC. (2023). https://github.com/s-andrews/FastQC.
75. Langmead B, and Salzberg SL (2012). Fast gapped-read alignment with Bowtie 2. Nat. Methods 9, 357–359. 10.1038/nmeth.1923. [PubMed: 22388286]
76. Li H. (2011). A statistical framework for SNP calling, mutation discovery, association mapping and population genetical parameter estimation from sequencing data. Bioinformatics 27, 2987–2993. 10.1093/bioinformatics/btr509. [PubMed: 21903627]
77. Raven KE, Blane B, Kumar N, Leek D, Bragin E, Coll F, Parkhill J, and Peacock SJ (2020). Defining metrics for whole-genome sequence analysis of MRSA in clinical practice. Microb. Genom 6, e000354. 10.1099/mgen.0.000354.
78. Lö ytynoja A, and Goldman N (2010). webPRANK: a phylogeny-aware multiple sequence aligner with interactive alignment browser. BMC Bioinf. 11, 579. 10.1186/1471-2105-11-579.
79. Garnier S, Ross N, Rudis R, Camargo PA, Sciaini M, and Cherer C. (2023). Viridis - Colorblind-Friendly Color Maps for R.

80. Wickham H, Navarro D, and Pedersen TL (2016). ggplot2: Elegant Graphics for Data Analysis (3e) (Springer-Verlag).

81. Gaupp R, Ledala N, and Somerville GA (2012). Staphylococcal response to oxidative stress. Front. Cell. Infect. Microbiol 2, 33. [PubMed: 22919625]

Highlights

- Staphyloxanthin production by *S. aureus* was elevated in non-healing diabetic wounds
- Staphyloxanthin enables *S. aureus* survival under oxidative conditions
- Murine diabetic wound healing is impaired by staphyloxanthin

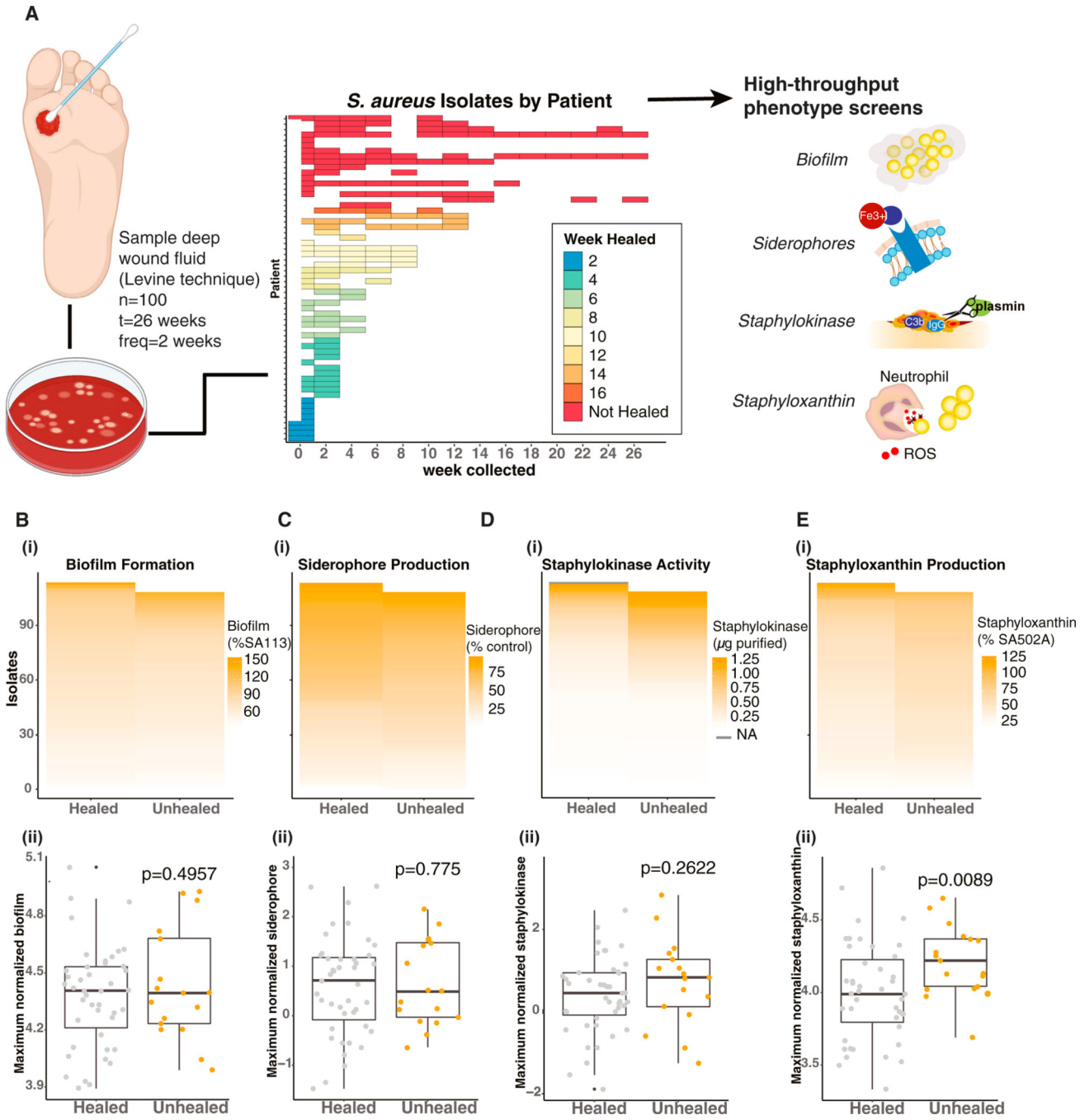

Figure 1. *Staphylococcus aureus* virulence phenotypes are associated with diabetic foot ulcer outcomes

(A) The Levine technique was used to collect swab specimens from diabetic foot ulcers (DFUs; n = 100) and cultured on selective agar to identify *S. aureus*. Of the 100 DFUs, 60 were culture positive for *S. aureus*. Variable virulence phenotypes were measured in all resulting isolates (n = 221) by high-throughput screens, where measures by isolate represent the means of 3 biological replicates by isolate averaged from 3 technical replicates each. (Bi, Ci, Di, and Ei) Distribution of phenotypes by isolate for all *S. aureus* isolates from healed (left) and unhealed (right) DFUs by the end of the 26-week study. (Bi) Biofilm

formation (percentage of *S. aureus* 113 mean), (Ci) siderophore production (percentage of absorbance$_{630}$ lost compared with untreated dye), (Di) staphylokinase activity (μg), and (Ei) staphyloxanthin production (percentage of *S. aureus* 502A mean).
(Bii, Cii, Dii, and Eii) Distribution of normalized virulence factor production (y axis) by a single representative isolate per DFU, as chosen by the isolate with the highest virulence factor production for each DFU, healed (left) and unhealed (right) by study end. p values are reported from t tests on maximum isolate phenotype value per DFU ~ healing outcome (n = 60 DFUs) for (Bii) log-normalized biofilm formation, (Cii) order quantile-normalized siderophore production, (Dii) order quantile-normalized staphylokinase activity, and (Eii) log-normalized staphyloxanthin production.
See Table S3 and Figure S1 for additional statistical analyses.

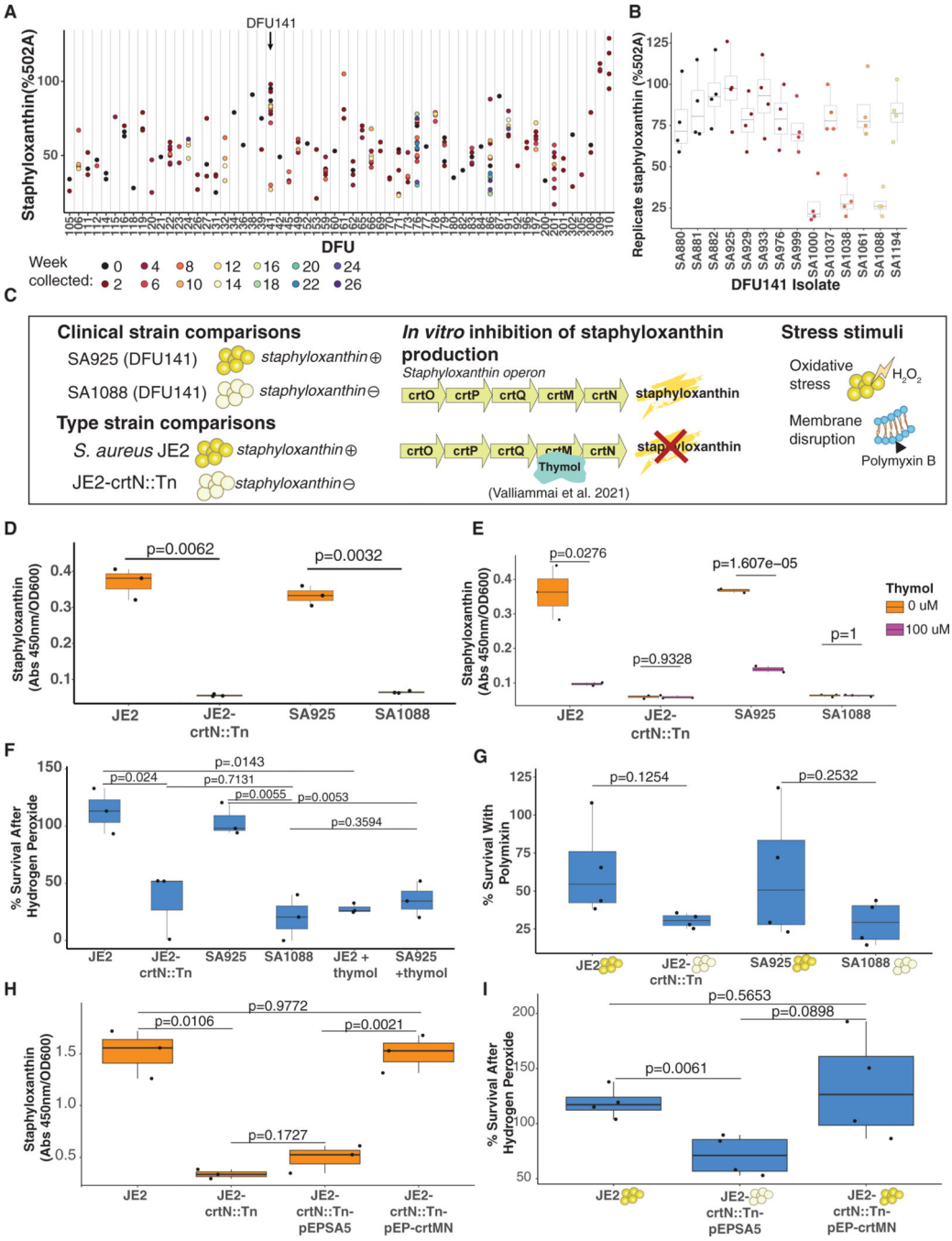

Figure 2. Staphyloxanthin promotes *S. aureus* growth and survival under oxidative stress

(A) Distribution of staphyloxanthin production (y axis) from all individual isolates cultured from each DFU (x axis), with DFU141 highlighted.

(B) Staphyloxanthin production (percentage of 502A) of each isolate cultured from DFU141 for each of three biological replicates (x axis).

(C) Schematic of comparison strains and conditions in (D) and (E).

(D) Staphyloxanthin production (mean Abs_{450}/OD_{600} across technical replicates) for 3 biological replicates of each comparator strain.

(E) Staphyloxanthin production in each strain with (right) and without (left) the addition of 100 μM thymol.

(F) Percentage of survival of JE2, JE2-crtN::Tn, SA925, and SA1088 strains treated with 3% H_2O_2.

(G) Percentage of survival following polymyxin B treatment.

(H) Staphyloxanthin production (absorbance$_{450}$/OD$_{600}$) in (from left to right) background strain (JE2), *crtN* transposon mutant (JE2-crtN::Tn), *crtN* mutant with an empty vector (JE2-crtN::Tn/pEPSA5), and the *crtN* mutant with *crtMN* complementation (JE2-crtN::Tn/pEP-crtMN) showing restored staphyloxanthin production.

(I) Percentage of survival (relative to dPBS vehicle) following 0.3% H_2O_2 exposure in JE2, JE2-crtN::Tn/pEPSA5, and complemented mutant JE2-crtN::Tn/pEPcrtMN. Independent t tests were performed to compare pairs of isolates.

(A–H) Each dot represents the mean of 3 technical replicates for 1 biological replicate. See also Figure S2.

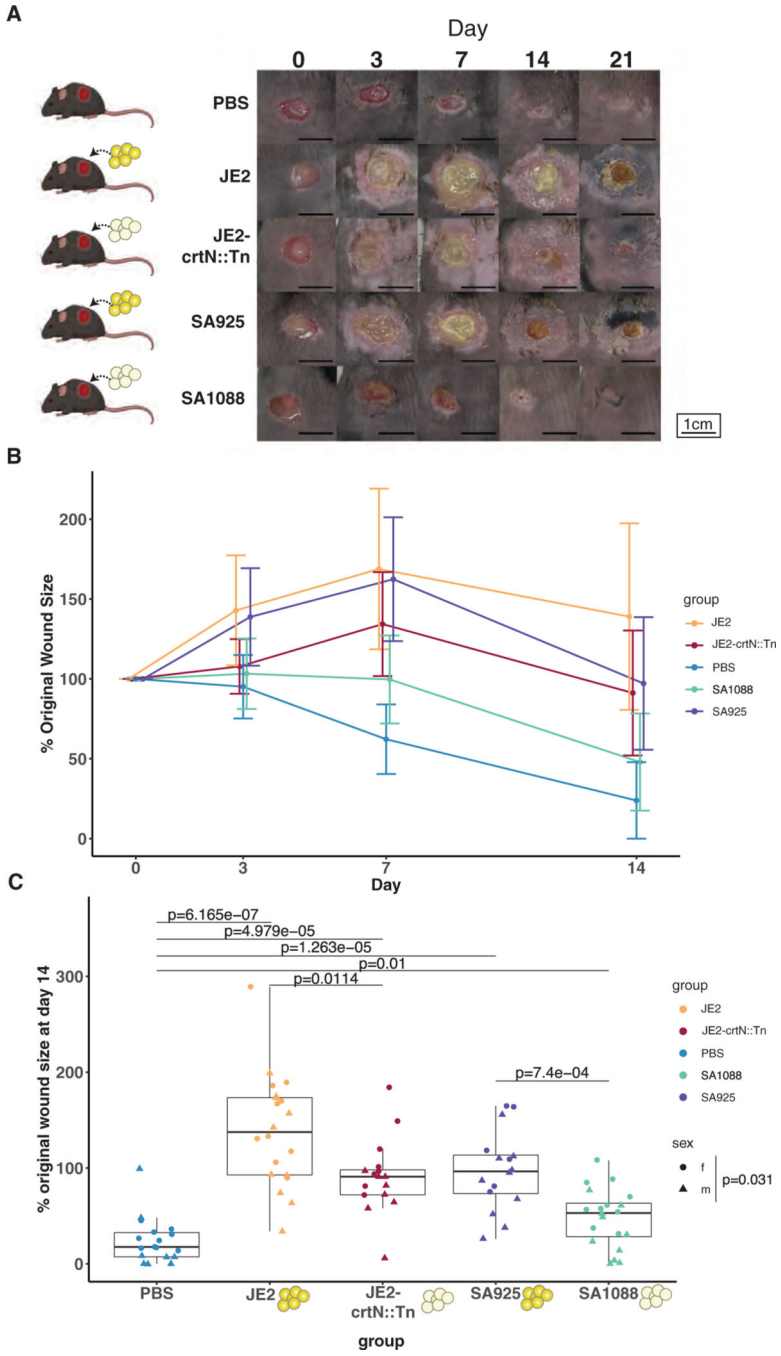

Figure 3. Staphyloxanthin delays wound healing in a diabetic mouse

(A) Full-thickness excisional wounds of male diabetic mice (db/db) were infected with 2×10^8 *S. aureus* each, with strains JE2, JE2-crtN::Tn, SA925, SA1088, or PBS control. Wound size was monitored for 21 days. Image rows follow one representative wound from each group. Scale bars represent 1 cm

(B) Relative wound size (percentage of original area) for days 0, 3, 7, and 14 by treatment group, where dots represent the mean within the group, and error bars represent mean ± standard deviation.

(C) Percentage of change in wound size (y axis) at day 14 post-wounding and infection by the *S. aureus* strains indicated above. Male (triangles) and female (circles) mice are indicated, where each triangle/circle represents the mean of 3 area measurements for each wound. Data represent two single sex-independent experiments. A two-sided Wilcoxon rank-sum test was performed among each group.
See also Figure S3.

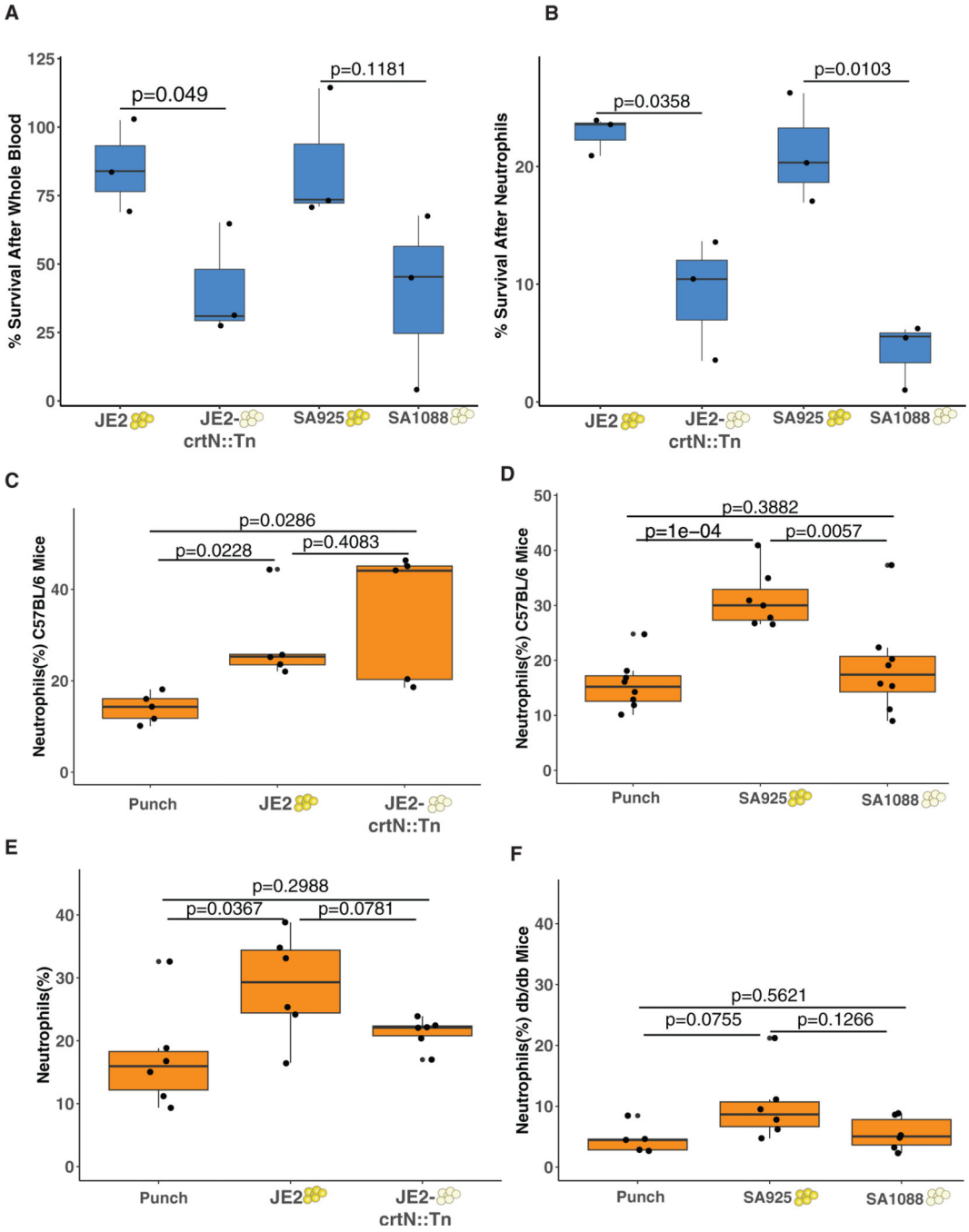

Figure 4. Staphyloxanthin production influences neutrophil survival and neutrophil recruitment in *S. aureus*

(A) Survival of each *S. aureus* strain when exposed to freshly drawn whole human blood for 4 h.

(B) Percentage of survival of each *S. aureus* strain when exposed to primary human neutrophils for 30 min.

(C−F) Flow cytometry results for ear punch wounds infected with 2×10^8 *S. aureus* strains, showing percentage of CD11b+ cells that stained Ly6G+ in ear pinnae from C57BL6/J (C and D) and diabetic db/db (E and F) mice. Each dot represents a mouse. Groups were

compared using independent t test. Each dot represents an independent experiment from a different donor.

See also Table S4

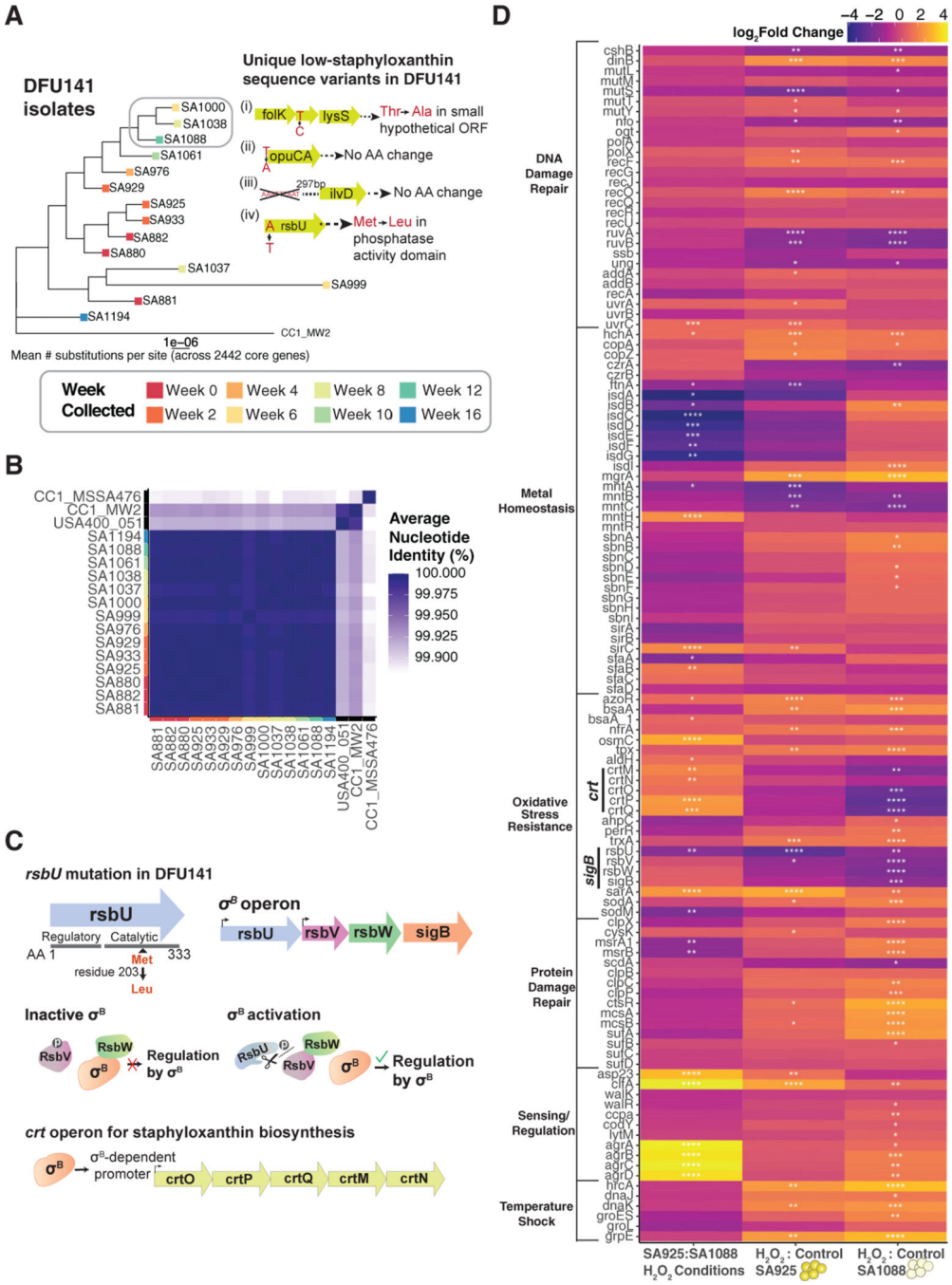

Figure 5. Genetic and transcriptomic analysis of high- and low-staphyloxanthin-producing clinical isolates

(A) (i) Maximum likelihood core gene phylogeny of all isolates collected from DFU141, with staphyloxanthin-deficient isolates circled. The CC1_MW2 outgroup branch is scaled down by 1/20 for visualization. The inset box depicts the four unique sequence variants shared by all three and their predicted amino acid changes.

(B) Average nucleotide identities between the 14 isolates from DFU141 and three clonal complex 1 (USA400) reference genomes showing strong genetic similarity between the DFU141 isolates. Isolates in both panels are labeled by the week they were collected.

(C) A single nucleotide change was identified in *rsbU* as the likely cause of low staphyloxanthin production in SA1088. RsbU is a regulator and part of the sigma B operon. Sigma B regulates staphyloxanthin biosynthesis.
(D) Expression of selected stress response genes (y axis) of SA1088 and SA925 with and without H_2O_2 (x axis). *log2 fold change $p < 0.05$.
See also Figure S5B.

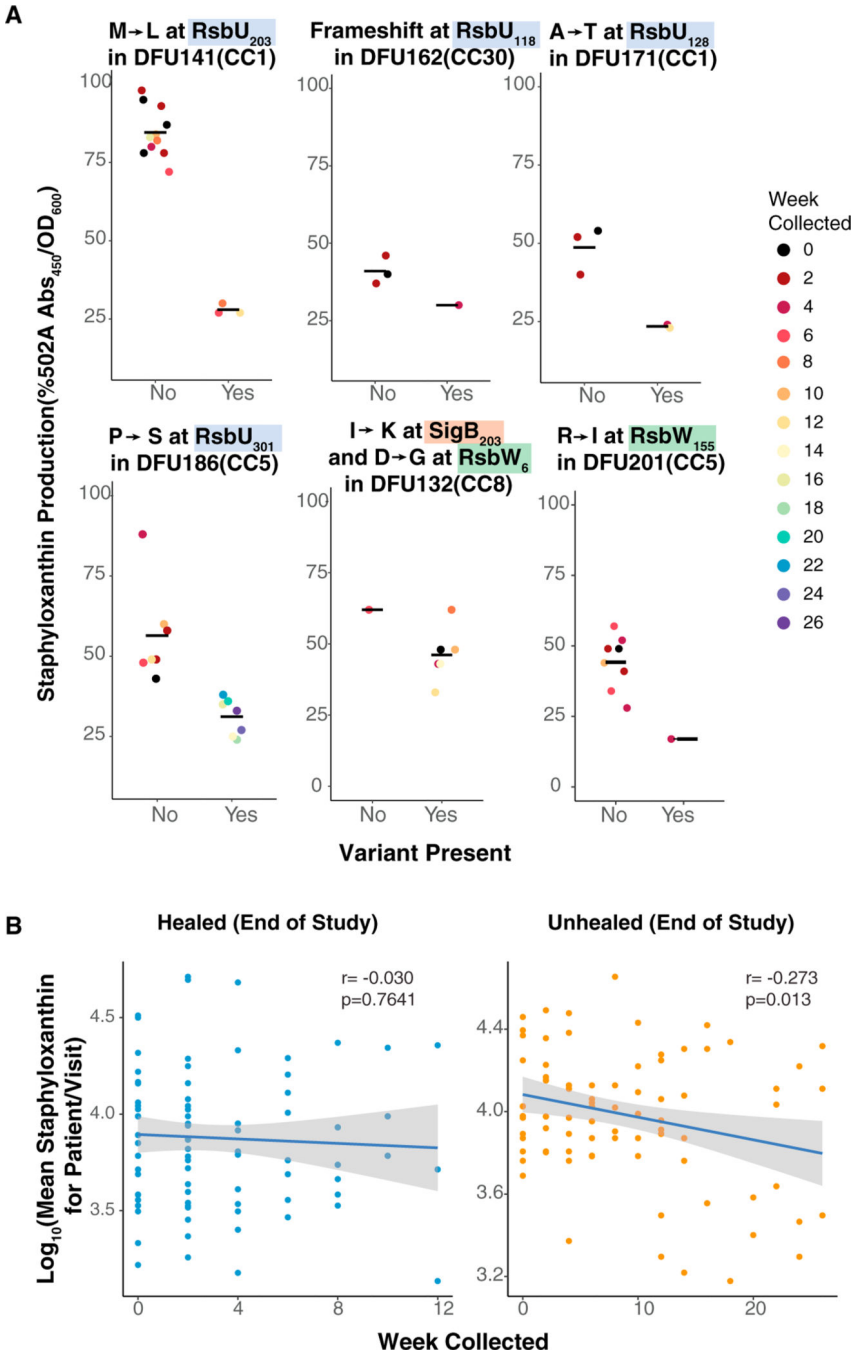

Figure 6. Loss-of-function mutations in the sigma B operon may be a convergent source of variation in staphyloxanthin production during DFU infection

(A) Staphyloxanthin production in isolates collected longitudinally from the same DFU and with and without non-synonymous variants in the sigma B operon, subset to examples where variants are associated with lower staphyloxanthin production.

(B) Correlations between staphyloxanthin and time in isolates from healing vs. non-healing DFUs. Staphyloxanthin measures were averaged across isolates for each patient within each

visit and then plotted by week collected. Pearson's correlation was calculated within the healed (n = 84 patient/time point combinations) and unhealed (n = 82) subsets.

KEY RESOURCES TABLE

REAGENT or RESOURCE	SOURCE	IDENTIFIER
Antibodies		
PerCP/Cyanine 5.5 anti-mouse CD8b (Ly-3)	BioLegend	Cat#126609; RRID:AB_961304
Brilliant Violet 421 anti-mouse/human CD11b (M1/70)	BioLegend	Cat#101235; RRID: AB_11203704
Brilliant Violet 605 anti-mouse CD90.2 (30-H12)	BioLegend	Cat#105343; RRID:AB_2632889
APC anti-mouse Ly-6G (1A8)	BioLegend	Cat#127613; RRID:AB_1877163
PE rat anti-mouse F4/80 (T45–2342)	BD Biosciences	Cat#565410; RID:AB_2687527
Mouse CD4 PE-Texas Red Conjugate	Invitrogen	Cat#MCD0417; RRID:AB_1474397
Brilliant Violet 785 anti-mouse Ly-6C (HK1.4)	BioLegend	Cat#128041; RRID:AB_2565852
FITC anti-mouse CD45.1 (A20)	BioLegend	Cat#110706; RRID:AB_313494
LIVE/DEAD Fixable Aqua Dead Cell Stain Kit 504 nm excitation	Invitrogen	Cat#34957
Bacterial and virus strains		
Staphylococcus aureus 502A	ATCC	Cat#27217
Staphylococcus arueus SA113	ATCC	Cat#35556
Staphylococcus aureus JE-2	BEI Resources	Cat#NR-46543
Staphylococcus aureus JE2-ΔcrtN	BEI Resources	Cat#NR-46925
Staphylococcus aureus JE2-ΔcrtN/pEPSA5	This paper	EGM7–08
Staphylococcus aureus JE2-ΔcrtM/pEP-CrtMN	This paper	EGM7–10
Staphylococcus aureus SA925	This paper	EGM5–76
Staphylococcus aureus SA1088	This paper	EGM5–77
E. coli IMO8	Monk et al.[36]	IMO8
Chemicals, peptides, and recombinant proteins		
Chloramphenicol	RPI	Cat#C61000–25
Blood agar	Remel	Cat#R01201
Tryptic soy broth, Difco	Fisher Scientific	Cat#DF0370
Bovine fibronectin	Sigma Aldrich	Cat#F1141
Cyrstal Violet	Sigma Aldrich	Cat#C6158
glu-plasminogen, human	Invitrogen	Cat#RP-43078

REAGENT or RESOURCE	SOURCE	IDENTIFIER
Chromogenix S-2251 (H-D-Valyl-L-leucyl-L-lysinep-Nitroaniline dihydrochloride)	Diapharma	Cat#S820332
Chromeazurol S	Sigma Aldrich	Cat#199532
Hydrogen peroxide solution 30% (w/w)	Sigma Aldrich	Cat#H1009
Polymyxin B	Sigma Aldrich	Cat#1547007
RPMI 1640	Invitrogen	Cat#11875085
Liberase TL	Roche	Cat#5401020001
DNase I	Sigma Aldrich	Cat#DN25
Neutrophil isolation medium (Lympholyte-poly cell separation media)	Cedarlane	Cat#CL5070
Red blood cell lysis buffer	Roche	Cat#11814389001
Gentamicin	Invitrogen	Cat#15750060
Trizol	Ambion Inc	Cat#15596026
BBL CHROMagar Staph aureus	BD	Cat#214982
Critical commercial assays		
Quick-DNA Miniprep Plus Kit	Zymo Research	Cat#D4069
Monach HMW DNA Extraction Kit for Tissue	NEB	Cat#T3060L
Direct-zol RNA MiniPrep Plus kit	Zymo Research	Cat#R2071
RNA 6000 Pico Kit	Agilent	Cat#50671513
Qubit™ RNA Broad Range Assay kit	Invitrogen	Cat#Q10211
Illumina Stranded Total RNA Prep with Ribo-Zero Plus	Illumina	Cat#20040529
IDT for Illumina UD indexes Set A	Illumina	Cat#20091655
DNA 1000 Kit	Agilent	Cat#5067–1504
dsDNA HS (High Sensitivity) Assay Kit	Invitrogen	Cat#Q32851
NextSeq 500/550 Mid Output Kit v2.5 (150 Cycles)	Illumina	Cat#20024904
Deposited data		
Pure culture RNASeq of SA925 and SA1088 with and without H2O2 exposure(11 total samples from 4 strain/condition combinations)	This paper	Bioproject: PRJNA1015705 SRA
Whole genome sequence assemblies of 220 isolates	This paper	Bioproject: PRJNA1015705
Experimental models: Organisms/strains		
C57BL6/J Mice	The Jackson Laboratory	Cat#000664

REAGENT or RESOURCE	SOURCE	IDENTIFIER
B6.BKS(D)-Leprdb/J Mice	The Jackson Laboratory	Cat#000697
Oligonucleotides		
CAGGAATTCAATGGCATTTCAATATAGGAG	This paper	20221121A
ATCGGGATCCCTCACATCTTTCTCTTAGAC	This paper	20221121B
ACACAATTTAACCCAGACGCT	This paper	20230113A
GAGACCCCACACTACCATCG	This paper	20230119A
Recombinant DNA		
pEPSA5	Forsyth et al.[35]	pEPSA5
pEP-CrtMN	This paper	EGM7–04
Software and algorithms		
Unicycler	Wick et al.[63]	https://github.com/rrwick/Unicycler
Porechop	R. Wick[64]	https://github.com/rrwick/Porechop
RaxML	Stamatakis et al.[65]	https://cme.h-its.org/exelixis/web/software/raxml/
PGAP	Haft et al.[46]	https://www.ncbi.nlm.nih.gov/genome/annotation_prok/
Mash	Ondov et al.[66]	https://github.com/marbl/Mash
Samtools	htslib.org	https://www.htslib.org/
Anvio	Eren et al.[67]	https://anvio.org/
Prokka	Seemann[43]	https://github.com/tseemann/prokka
Roary	Page et al.[44]	https://sanger-pathogens.github.io/Roary/
Trim galore	Kreuger[68]	https://www.bioinformatics.babraham.ac.uk/projects/trim_galore/
DESeq2	Love et al.[69]	https://bioconductor.org/packages/release/bioc/html/DESeq2.html
Rsubread	Liao et al.[70]	https://bioconductor.org/packages/release/bioc/html/Rsubread.html
BLASTP	NCBI	https://blast.ncbi.nlm.nih.gov/Blast.cgi
ImageJ	National Institute of Health	https://imagej.nih.gov/ij/
Other		
Punch Biopsy Punch	Integra Miltex	Cat#33–37

REAGENT or RESOURCE	SOURCE	IDENTIFIER
DietGel Recovery	Clear H2O	Cat#72–06-5022
Sterile swabs	Puritan	Cat#25–1506 1PF
40 μm cell strainer	Falcon	Cat#352340
MiniBeadbeater 16	BioSpec	Cat#607
Zirconia/silica beads, 0.1 mm	BioSpec	Cat#11079101z
2100 Bioanalyzer Instrument	Agilent	Cat#G2939BA
Qubit 2.0 Fluorometer	Life Technologies	Cat#Q32866